MELASにおけるQOLと脳卒中発作の関係

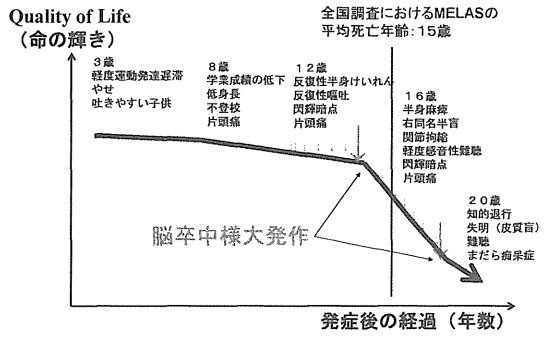

臨床症状	投与前の発現例数	改善率＊（改善例/発現例）の推移				
		15分	30分	2時間	6時間	1日
頭痛	22	0% (0/22)	64%＊ (14/22)	100%＊ (22/22)	100%＊ (22/22)	100%＊ (22/22)
臨床的障害	22	14% (3/22)	14% (3/22)	100%＊ (22/22)	100%＊ (22/22)	100%＊ (22/22)
嘔気	8	0% (0/8)	75%＊ (6/8)	100%＊ (8/8)	100%＊ (8/8)	100%＊ (8/8)
嘔吐	10	0% (0/10)	70%＊ (7/10)	100%＊ (10/10)	100%＊ (10/10)	100%＊ (10/10)
一過性失明	7	43% (3/7)	29% (2/7)	100%＊ (7/7)	100%＊ (7/7)	100%＊ (7/7)
半身痙攣	5	46% (2/5)	60% (3/5)	100%＊ (5/5)	100%＊ (5/5)	100%＊ (5/5)
意識障害	1	0% (0/1)	100% (1/1)	100% (1/1)	100%＊ (1/1)	100%＊ (1/1)
閃輝暗点	9	0% (0/9)	67%＊ (6/9)	89%＊ (8/9)	100%＊ (9/9)	100%＊ (9/9)

＊：p<0.05 by Fisher's exact test.　Koga Y et al. Neurology 64:710-715, 2005

頻回発作型MELASでのL-アルギニン内服による発作予防

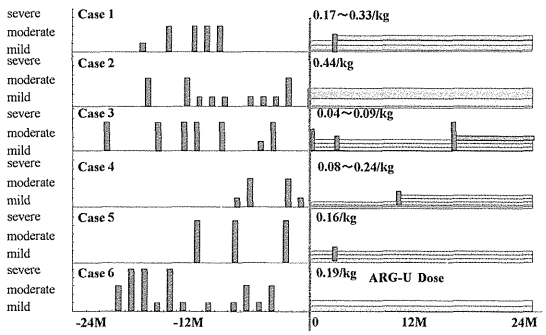

Koga Y et al. Neurology 64:710-715, 2005 Highlighting paper

Department of Pediatrics and Child Health, Kurume University School of Medicine

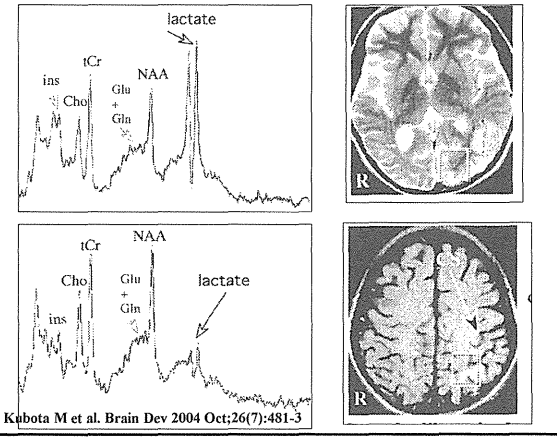

Kubota M et al. Brain Dev 2004 Oct;26(7):481-3

アルギニンによる血管内皮機能の改善

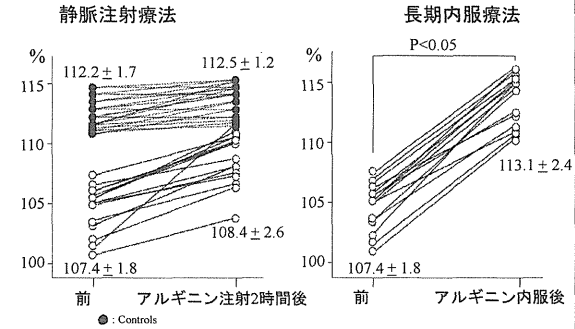

Koga Y et al. Neurology 66:1766-1769, 2006

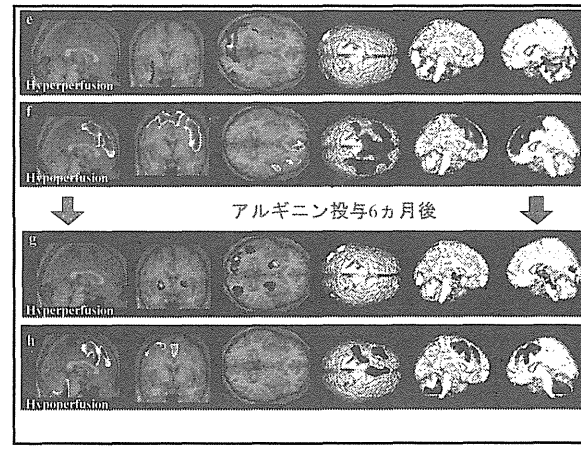

INTERNAL MEDICINE

ORIGINAL ARTICLE

Taurine Ameliorates Impaired the Mitochondrial Function and Prevents Stroke-like Episodes in Patients with MELAS

Mitsue Rikimaru[1], Yutaka Ohsawa[1], Alexander M. Wolf[2], Kiyomi Nishimaki[2], Harumi Ichimiya[2], Naomi Kamimura[2], Shin-ichiro Nishimatsu[3], Shigeo Ohta[2] and Yoshihide Sunada[1]

Abstract

Objective Post-transcriptional taurine modification at the first anticodon ("wobble") nucleotide is deficient in A3243G-mutant mitochondrial (mt) $tRNA^{Leu(UUR)}$ of patients with myopathy, encephalopathy, lactic acidosis, and stroke-like episodes (MELAS). Wobble nucleotide modifications in tRNAs have recently been identified to be important in the accurate and efficient deciphering of codons. We herein examined whether taurine can alleviate mitochondrial dysfunction in patient-derived pathogenic cells and prevent clinical symptoms in MELAS patients.

Methods and Results The addition of taurine to the culture media ameliorated the reduced oxygen consumption, decreased the mitochondrial membrane potential, and increased the oxidative stress in MELAS patient-derived cells. Moreover, high dose oral administration of taurine (0.25 g/kg/day) completely prevented stroke-like episodes in two MELAS patients for more than nine years.

Conclusion Taurine supplementation may be a novel potential treatment option for preventing the stroke-like episodes associated with MELAS.

Key words: MELAS, post-transcriptional modification, taurine, stroke-like episodes

(Intern Med 51: 3351-3357, 2012)
(DOI: 10.2169/internalmedicine.51.7529)

Introduction

An A3243G or T3271C transition in the mitochondrial (mt) $tRNA^{Leu(UUR)}$ gene has been identified in approximately 80% and 10% respectively, of patients with mitochondrial myopathy, encephalopathy, lactic acidosis, and stroke-like episodes (MELAS) (1). Nearly 90% of patients with myoclonus epilepsy associated with ragged-red fibers (MERRF) possess an A8344G transition in the mt $tRNA^{Lys}$ gene (1). These mutations are located in the cloverleaf structure of each mt tRNA. However, it remains unknown how such point mutations in mt tRNAs induce mitochondrial dysfunction leading to the wide variety of MELAS or MERRF symptoms.

Post-transcriptional modifications in tRNAs play critical roles in modifying the genetic code. In 1966, Francis Crick proposed that the first anticodon ("wobble") nucleotide recognizes the third codon nucleotide through non-canonical Watson-Crick geometry; so-called "wobble" pairing (2). Growing evidence has shown that various post-transcriptional modifications at the wobble nucleotides in tRNAs are required to recognize their cognate codons accurately and efficiently (3). In normal human mt $tRNA^{Leu(UUR)}$ or mt $tRNA^{Lys}$, uridine at the wobble position is modified with taurine, a sulfur-containing β-amino acid (4-6). In contrast, the taurine modification is deficient in mutant mt $tRNA^{Leu(UUR)}$ or mutant mt $tRNA^{Lys}$ derived from clinical specimens of MELAS or MERRF patients (4-8). The taurine modification defect in the mutant mt tRNAs causes a deficiency in deciphering codons (1, 9). These findings have given rise to the intriguing possibility that MELAS and

[1]Department of Neurology, Kawasaki Medical School, Japan, [2]Department of Biochemistry and Cell Biology, Institute of Development and Aging Sciences, Nippon Medical School, Japan and [3]Department of Molecular and Developmental Biology, Kawasaki Medical School, Japan
Received for publication February 13, 2012; Accepted for publication August 6, 2012
Correspondence to Dr. Yoshihide Sunada, ysunada@med.kawasaki-m.ac.jp

MERRF are tRNA-modification disorders associated with the impairment of correct mitochondrial gene translation.

We hypothesized that high-dose taurine supplementation could restore the taurine modification of the mutant tRNAs in MELAS or MERRF patients. In the current study, we explored the potential therapeutic effect of taurine by examining the mitochondrial functions in patient-derived pathogenic cells and by observing the clinical symptoms in MELAS patients receiving taurine supplements.

Materials and Methods

The local ethics committee approved this study (No. 787) and all patients gave their informed consent for participation.

Construction of cybrid cells harboring mutant mtDNA

Immortalized cells possessing patient-derived mitochondrial (mt) DNA were constructed by the intercellular transfer of a patient's mtDNA to ρ^0 HeLa cells (EB8), which are mtDNA-less immortalized cells (10). EB8 cells were isolated by the long-term treatment of HeLa cells with ethidium bromide. Primary dermal fibroblasts were isolated from skin biopsy samples from an A3243G-MELAS, a T3271C-MELAS, and an A8344G-MERRF patient. The fibroblasts were enucleated by centrifugation in the presence of cytochalasin B. Then, the enucleated fibroblasts were fused with EB8 cells by treatment with polyethylene glycol. Control cytoplasmic hybrid (cybrid) strains (Ft2-11, A2) were constructed by fusing mtDNA-less HeLa cells with enucleated normal human fibroblasts.

The resulting cybrids were maintained in Dulbecco's modified Eagle's medium/Ham's F12 medium supplemented with 10% fetal bovine serum, 1 mM sodium pyruvate, 50 μg uridine, 100 units/mL penicillin, and 100 μg/mL streptomycin (Invitrogen/Life Technologies Japan, Tokyo, Japan). Cybrids with more than 95% mutant mtDNA were used for the experiments. To decrease the endogenous taurine, the cells were also cultured in media with limited amounts of the taurine precursor, L-cysteine (1 mg/mL), and the taurine intermediate, L-methionine (high glucose, L-glutamine-minus, sodium pyruvate-minus Dulbecco's modified Eagle's medium; Gibco) supplemented with L-glutamine, sodium pyruvate, and uridine. The growth rate of mutant cybrids was unchanged after culture in limiting media for seven days.

Cell lines and in vitro analyses

Primary dermal fibroblasts obtained from skin biopsy samples from an A3243G-MELAS, a T3271C-MELAS, and an A8344G-MERRF patient were enucleated and subsequently fused with mt DNA-less HeLa cells (10). The resulting cybrid cells were treated with or without taurine and then were used in subsequent *in vitro* analyses of the mitochondrial oxygen consumption (11), membrane potential (12), and reduction and oxidation (redox) status (10). Taurine powder was purchased from Taisho Pharmaceutical Co., Ltd. (Tokyo, Japan).

Mitochondrial oxygen consumption

Cybrid cells cultured with or without taurine were trypsinized and resuspended in serum-free medium. The cell suspension was continuously stirred at 37℃ with an oxygen electrode (11). The cell concentration was determined using a hemocytometer. The oxygen consumption rates were measured using an Oxygen Meter Model 781 and a Mitocell MT200 closed respiratory chamber (Strathkelvin Instruments, North Lanarkshire, UK). The oxygen respiration rate was directly measured for the 40 mM taurine experiments. After treatment with the limiting media described above, the oxygen consumption was examined in the presence of 1 μM carbonyl cyanide p-trifluoromethoxyphenylhydrazone (FCCP), a mitochondrial protonophore used to measure electron transport activity. The consumption value was subtracted from the 1 mM potassium cyanide-independent oxygen consumption value.

Mitochondrial membrane potential

To evaluate the mitochondrial membrane potential, cybrid cells were incubated for 30 minutes at 37℃ with 20 nM MitoTracker Red (Molecular Probes, Invitrogen, Carlsbad, CA, USA), a red-fluorescent dye that accumulates at the mitochondrial membrane (12) in response to the membrane potential. The MitoTracker Red signal increases in a membrane potential-dependent manner. The images were visualized with a confocal laser-scanning microscope (Fluoview FV300; Olympus, Tokyo, Japan) at an excitation wavelength of 594 nm. For the flow cytometric analysis, cells stained with MitoTracker Red were washed in phosphate-buffered saline, trypsinized, and analyzed using a Cell Lab Quanta™ instrument (Beckman Coulter, Inc., Brea, CA, USA). The fluorescent signal of more than 10,000 cells was examined for each experiment.

Mitochondrial redox status

The redox-sensitive green fluorescent protein, roGFP1, generates a unique fluorescence image after the formation (oxidation) of the disulfide bonds adjacent to the barreled β-sheets in the GFP protein (11). To allow real-time visualization of mitochondrial redox status, cybrid cells were stably transfected with the roGFP1 expression vector containing a mitochondrial-targeting sequence. Fluorescence images were recorded using a multi-dimensional imaging workstation (AS MDW; Leica Microsystems, Wetzlar, Germany) consisting of a tunable light source (Polychrome IV monochromator; Till Photonics, Gräfelfing, Germany), an inverted epifluorescence microscope (DM IRE2; Leica Microsystems) contained in a climate chamber maintained at 37℃, and a cooled charge-coupled device camera (CoolSnap HQ; Roper Scientific, Princeton, NJ, USA). The dual excitation ratio of roGFP1 from a single cell was recorded. The ratio of the reduced form of roGFP1 (roGFP1-SH) to the oxidized form

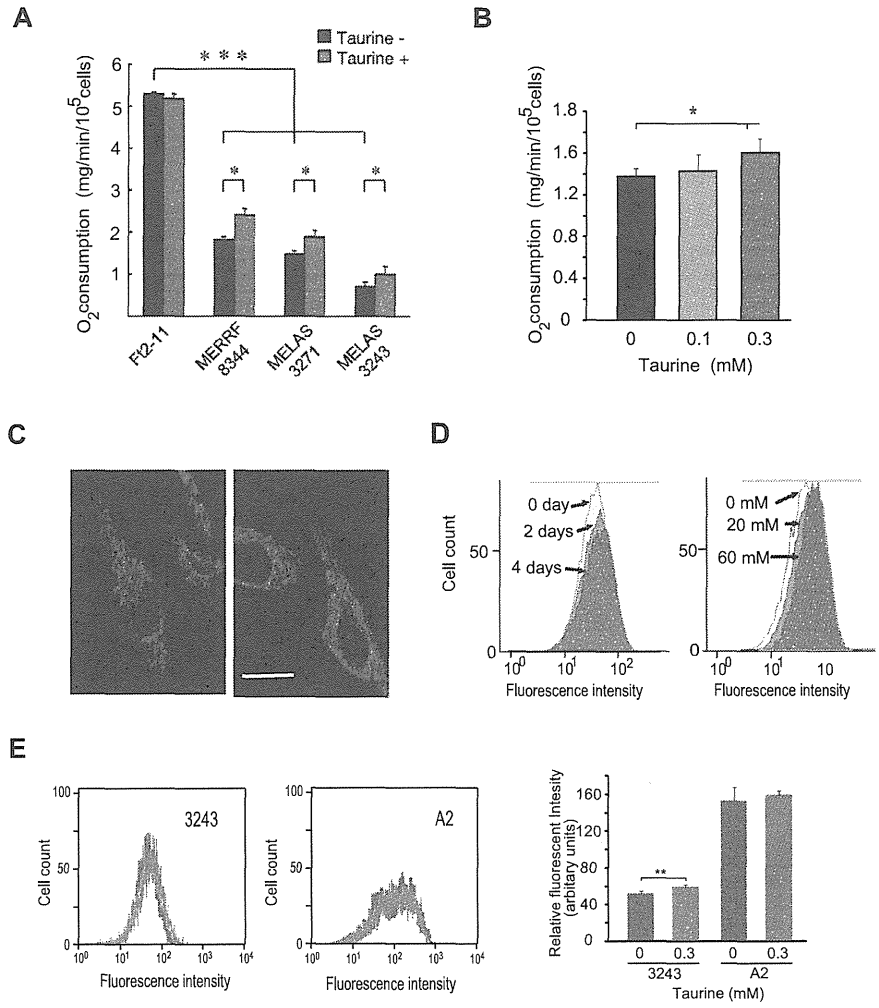

Figure 1. **Taurine ameliorates the impaired mitochondrial function in patient-derived cybrid cells. (A) Patient-derived cybrid cells showed marked decreases in oxygen consumption (black bars). After four days in culture with taurine (40 mM), there was a significant increase in the oxygen consumption rates in patient-derived cybrids with mutant mtDNA, but not in wild-type control Ft2-11 cells (red bars) (*p < 0.05). (B) Cybrids were cultured in media with limited amounts of the taurine intermediate, L-methionine (1 mg/mL), and the taurine precursor, L-cysteine (5 mg/mL), for two days, followed by an additional four day culture with or without taurine (0, 0.1, or 0.3 mM). Taurine (0.3 mM) improved the oxygen consumption in the A3243G-MELAS cybrids cultured in the limiting media (*p < 0.05). (C) Cybrids were cultured in the presence (right) or absence (left) of 40 mM taurine for 4 days. Staining with the membrane potential-sensitive red-fluorescent dye MitoTracker Red (100 nM for 30 min) revealed an increased mitochondrial membrane potential with morphological improvement in the A3243G-MELAS cybrid cells. Scale bar: 100 μm. (D) The mitochondrial membrane potential was determined by a flow cytometric analysis after staining with 100 nM of MitoTracker Red for 30 min. The profiles in the left-hand panel show a time-dependent increase in membrane potential after incubation with 40 mM taurine. The right-hand profiles indicate that there was a dose-dependent shift in the membrane potential after four days of culture with the indicated amounts of taurine. (E) Cybrid cells were cultured in the limiting media described in (B). The reduced mitochondrial membrane potential in the A3243G-MELAS cybrid cells (3243) was significantly improved as judged by a flow cytometric analysis after a four-day incubation with 0.3 mM taurine (*p < 0.05). In contrast, the membrane potential in the control cybrid cells (A2) was unchanged after taurine treatment.**

of roGFP1 (roGFP1-SS-) was obtained. The fluorescence ratio at 410:490 nm was used as the index of oxidation (11).

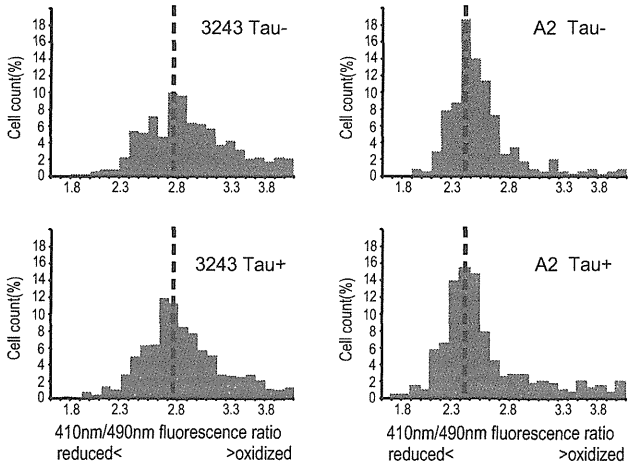

Figure 2. Taurine reduces the oxidative stress in patient-derived cybrid cells. The A3243G-MELAS cybrid cells (3243, left) and the control cybrid cells (A2, right) were stably transfected with a mitochondria-targeting redox-sensitive green fluorescent protein (roGFP). The histograms show the distribution of cells according to their 410:490 nm fluorescence ratio, an indicator of the oxidation status. Compared with the A2 cybrid cells, the ratio was increased in the 3243 cybrid cells, suggesting an increase in oxidative stress (green, upper) The addition of taurine (3 mM; red, lower) caused a shift towards a reduced status in the 3243 cybrid cells, but not in the A2 cybrid cells (red, lower). The data represent the mean values from eight independent experiments. *p < 0.05 between culture conditions with and without taurine.

Oral administration of taurine to patients with A3243G-MELAS

Taurine powder was orally administered three times a day, after a meal, to two patients with A3243G-MELAS at a dose of 0.25 g/kg/day. This corresponds to the maximal dose previously employed for Japanese patients with biliary obstructions (13).

Statistical analyses

Paired observations were statistically analyzed using a one-way analysis of variance followed by Bonferroni's test. p values <0.05 were considered to be statistically significant.

Results

Taurine restores the reduced mitochondrial oxygen consumption in patient-derived cells

The cybrid cells harboring the disease-causing mutant mtDNAs showed lower oxygen consumption rates than the control cells (Fig. 1A). The addition of 40 mM taurine to the culture media increased the oxygen consumption rate in patient-derived cybrid cells, but not in control cells. Moreover, 0.3 mM taurine was also effective when the cybrid cells were cultured in limiting media lacking cysteine and methionine, which are a precursor and an intermediate, respectively, of taurine biogenesis (Fig. 1B).

Taurine improves the reduced mitochondrial membrane potential in A3243G-MELAS cells

MitoTracker Red-labeled mitochondria in the A3243G-MELAS cybrid cells displayed a weak signal with a granular appearance, suggesting that they had a decreased mitochondrial membrane potential compared to normal cells (Fig. 1C, left) (12). When the cybrid cells were cultivated in the presence of 40 mM taurine for four days, the mitochondria underwent changes in their morphology to a normal filamentous appearance, which was accompanied by an increase in the membrane potential (Fig. 1C, right) (12). The reduced mitochondrial membrane potential in the A3243G-MELAS cells was reversed by taurine in a time- and concentration-dependent manner (Fig. 1D). Moreover, 0.3 mM taurine increased the membrane potential in the A3243G-MELAS cybrids that were cultured in limiting media (Fig. 1E). In contrast, taurine did not alter the membrane potential in the control A2 cybrid cells.

Taurine improves the impaired redox status in patient-derived cells

We transfected the MELAS-cybrid cells with a gene encoding a redox-sensitive green fluorescent protein, roGFP, to monitor their redox status as judged by the ratio of fluorescence signals at 410 and 490 nm (11). The ratio in the A3243G-MELAS cybrid cells increased in comparison to that in the control cells, thus suggesting that they had an increased degree of oxidative stress (Fig. 2, upper). The addition of taurine to the culture media reduced the ratio in the A3243G-MELAS cybrid cells, but not in the control cells (Fig. 2, lower).

Taurine prevents stroke-like episodes in A3243G-MELAS patients

Case 1: A 29-year-old woman had an abrupt onset of generalized seizures and was admitted to our hospital in February 2001 (Fig. 3A). The lactate and pyruvate levels in her serum were elevated to 48.3 mg/dL (normal range, 3.0-17.0 mg/dL) and 1.7 mg/dL (normal range, 0.3-0.9 mg/dL), respectively. Brain magnetic resonance imaging (MRI) revealed a stroke-like lesion in the left occipital region (Fig. 3B). A biopsy from the left biceps brachii muscle showed a MELAS-like pattern, with cytochrome c oxidase-negative ragged-red fibers and succinate dehydrogenase-reactive blood vessels. A molecular genetic analysis of the mitochondrial DNA confirmed an A3243G transition. Treatment with coenzyme Q10 (180 mg daily) and phenytoin (250 mg daily) was commenced in February 2001. The anticonvulsant was switched from phenytoin to valproate (600 mg daily) in April 2001 because of repeated generalized seizures. A follow-up MRI in August 2001 revealed an additional right occipitotemporal lesion (Fig. 3C). The patient continued to experience epileptic seizures and had a stroke-

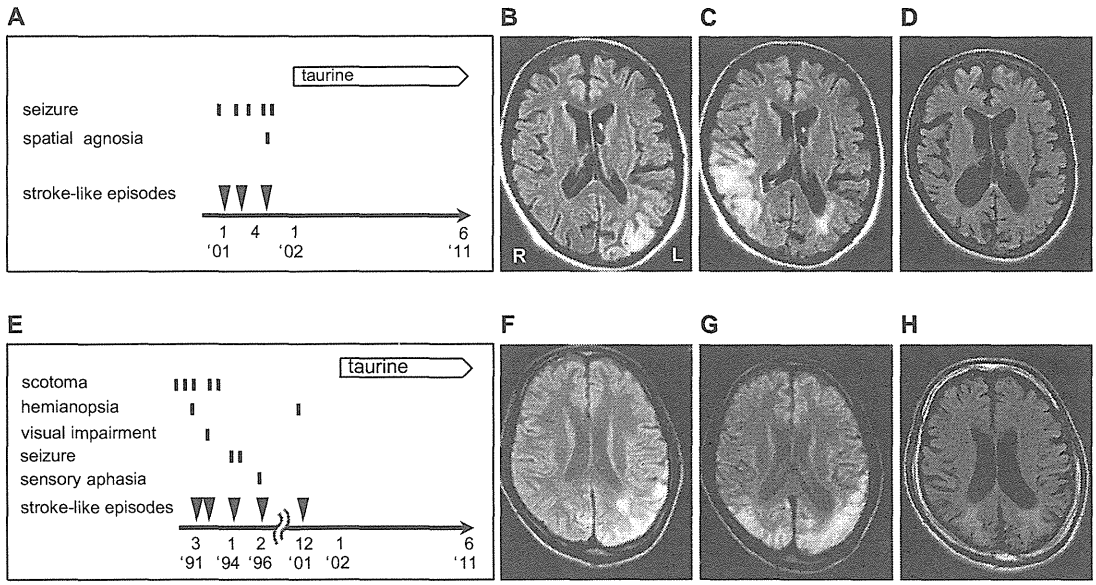

Figure 3. **Oral administration of taurine reduces the stroke-like episodes in MELAS patients. The clinical courses of two MELAS patients (Cases 1 and 2) harboring the A3243G mutation in the mt $tRNA^{Leu(UUR)}$ (A, E) are shown. Taurine administration completely prevented stroke-like episodes in both patients for more than nine years. Fluid Attenuated Inversion Recovery (FLAIR) images of brain MRI revealed that multiple stroke-like lesions had developed in the occipitotemporal region before oral taurine administration (B, C, F, G). The most recent MRI showed no additional stroke-like lesions after taurine treatment in both patients (D, H).**

like episode presenting hemispatial agnosia over the next seven months. Oral taurine supplementation was started in January 2002. From the beginning of the taurine treatment, her epileptic and stroke-like episodes ceased completely. In July 2007, her blood concentration of taurine was 481.3 μM, more than 5-fold higher than the normal range (39.5-93.2 μM). In December 2010, the elevated levels of serum lactate and pyruvate had declined to near normal levels, at 24.3 mg/dL and 0.9 mg/dL, respectively. The most recent brain MRI exhibited no new lesions, but mild cerebral atrophy was present (Fig. 3D). The patient has been doing well for the last nine years with the taurine treatment still ongoing.

Case 2: A 21-year-old man was admitted to another hospital in March 1991 because of repeated scintillating scotoma and right homonymous hemianopsia (Fig. 3E). He was diagnosed with A3243G-MELAS based on typical muscle biopsy findings and a mtDNA analysis. He was treated with coenzyme Q10 (120 mg/dL) and phenytoin (150 mg daily); however, he soon developed vision loss on the right side. He was admitted to our hospital in July 1991. The serum levels of lactate and pyruvate were elevated to 38.7 mg/dL and 1.2 mg/dL, respectively. The anticonvulsant was switched from phenytoin to valproate (600 mg daily) in January 1994 because of repeated generalized seizures. Over the next eight years he suffered from several stroke-like episodes, including sensory aphasia and visual impairment. Brain MRI scans in October 1991 and January 1994 revealed an accumulation of stroke lesions in the bilateral occipital regions (Fig. 3F, G). In December 2001 he had a stroke-like episode presenting with left hemianopsia. Taurine supplementation was started in January 2002, and since then, no stroke-like episodes have occurred. In September 2007, his blood taurine concentration was 996.0 μM, approximately 10-fold higher than the normal range. In February 2010, the serum values of lactate and pyruvate had declined to 29.1 mg/dL and 0.38 mg/dL, respectively. The most recent brain MRI exhibited no additional stroke-like lesions (Fig. 3H).

Discussion

Post-transcriptional modifications at the wobble nucleotide are crucial for the maturation mechanisms of tRNAs and they are required for the correct decoding of codons. In A3243G-MELAS patients, the taurine modification is defective at the wobble nucleotide in the mutant mt $tRNA^{Leu(UUR)}$ (5). In the present study, we showed that taurine ameliorates the mitochondrial dysfunction in patient-derived pathogenic cells carrying mutant $tRNA^{Leu(UUR)}$, but did not reinforce the normal mitochondrial function in control cells. Oral taurine administration also achieved long-term prevention of stroke-like episodes in two patients with MELAS.

We previously showed that when taurine (τ) is added to the culture media of HeLa cells, it is transported to the mitochondria and used as a substrate to synthesize taurine-modified uridine, 5-taunomethyluridine (τm^5U), in mt $tRNA^{Leu(UUR)}$ (Fig. 4A) (1, 4-7). Considering that τm^5U formation proceeds through an enzymatic reaction, the present results suggest that an increased concentration of taurine ac-

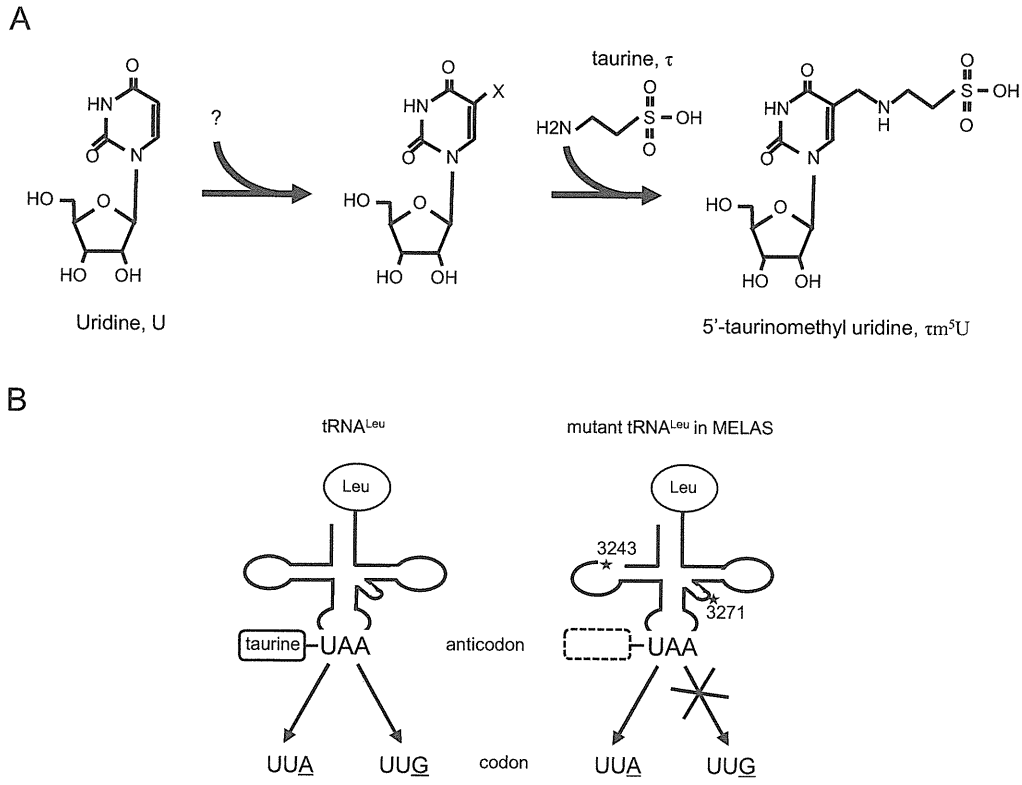

Figure 4. A proposed pathomechanism of MELAS, an RNA-modification disorder. (A) A mechanism of post-transcriptional taurine modification at the first wobble anticodon [uridine (U)] in normal mt tRNA$^{Leu(UUR)}$. Taurine (τ) is incorporated into the C5 position of the uracil ring to generate the final modification product, 5-taurinomethyluridine (τm^{5}U) (4). (B) Taurine modification functions to stabilize the wobble anticodon-codon pairing. Normal mt tRNA$^{Leu(UUR)}$, with a taurine-modification at the wobble uridine (U), efficiently pairs with codons UUA and UUG (right). In contrast, the MELAS-causing mutant mt tRNA$^{Leu(UUR)}$ lacks the wobble taurine modification, resulting in a specific reduction of UUG codon-specific translation but not UUA codon-specific translation. Defective taurine modification in the mutant mt tRNA$^{Leu(UUR)}$ results in a deficiency in mitochondrial protein synthesis caused by an inability to decipher codons (left) (7).

celerates the enzymatic formation of τm^{5}U, thereby reversing impaired codon recognition by the mutant mt tRNA$^{Leu(UUR)}$ (Fig. 4B). The pathogenic mutations in MELAS and MERRF might hinder the specific recognition by an RNA-modifying enzyme (4-7). Further studies will be required to clarify the precise molecular mechanisms underlying the wobble taurine modification in mt tRNA$^{Leu(UUR)}$, and how much supplemented taurine incorporates into the wobble uridine in mutant mt tRNA$^{Leu(UUR)}$ in clinical samples from patients.

Low plasma concentrations of taurine induce cardiomyopathy in cats. This particular species has no biosynthetic pathway for endogenous taurine (14). In agreement with our results, high-dose oral administration of taurine to cats increased the plasma and cardiac concentrations, and ameliorated the cardiac dysfunction. Because the cardiac muscles are composed of slow myofibers that are rich in mitochondria (14), taurine supplementation could alleviate the cardiomyopathy via increased τm^{5}U formation in mt tRNAs.

The present results provide new insight into our understanding of MELAS, and possibly MERRF, as putative RNA-modification disorders that lack the wobble taurine modification. Our results also suggest that the oral administration of taurine may be an effective therapy for these disorders.

The authors state that they have no Conflict of Interest (COI).

Acknowledgement

This work was supported by research grants for Intramural Neurological and Psychiatric Disorders from the National Center of Neurology and Psychiatry (20B-13, 23-5); by grants for Comprehensive Research on Disability Health and Welfare from the Ministry of Health, Labour and Welfare of Japan (H20-018); by Grants-in-Aid for Scientific Research from the Japan Society for the Promotion of Science (C-20591013, C-21591101, and C-23591261); and by research project grants from the Kawasaki Medical School (22-A24, 21-T1, 23-P601, 23-T1).

References

1. Suzuki T, Nagao A, Suzuki T. Human mitochondrial diseases caused by lack of taurine modification in mitochondrial tRNAs. WIREs RNA **2**: 376-386, 2011.
2. Click FHC. Codon-anticodon pairing: the wobble hypothesis. J Mol Biol **19**: 548-555, 1966.
3. Curran JF. Modified nucleosides in translation. In: Modification and Editing of RNA. Grosjean H, Benne R, Eds. ASM Press, Washington, D.C, 1998: 493-516.
4. Yasukawa T, Suzuki T, Ishii N, Ueda T, Ohta S, Watanabe K. Defect in modification at the anticodon wobble nucleotide of mitochondrial tRNA(Lys) with the MERRF encephalomyopathy pathogenic mutation. FEBS Lett **467**: 175-178, 2000.
5. Yasukawa T, Suzuki T, Ueda T, Ohta S, Watanabe K. Modification defect at anticodon wobble nucleotide of mitochondrial tRNAs (Leu)(UUR) with pathogenic mutations of mitochondrial myopathy, encephalopathy, lactic acidosis, and stroke-like episodes. J Biol Chem **275**: 4251-4257, 2000.
6. Yasukawa T, Suzuki T, Ishii N, Ohta S, Watanabe K. Wobble modification defect in tRNA disturbs codon-anticodon interaction in a mitochondrial disease. EMBO J **20**: 4794-4802, 2001.
7. Suzuki T, Nagao A, Suzuki T. Human mitochondrial tRNAs: biogenesis, function, structural aspects, and diseases. Annu Rev Genet **45**: 299-329, 2011.
8. Kirino Y, Goto Y, Campos Y, et al. Specific correlation between the wobble modification deficiency in mutant tRNAs and the clinical features of a human mitochondrial disease. Proc Natl Acad Sci USA **102**: 7127-7132, 2005.
9. Kirino Y, Yasukawa T, Ohta S, et al. Codon-specific translational defect caused by a wobble modification deficiency in mutant tRNA from a human mitochondrial disease. Proc Natl Acad Sci USA **101**: 15070-15075, 2004.
10. Hayashi J, Ohta S, Kikuchi A, et al. Introduction of disease-related mitochondrial DNA deletions into HeLa cells lacking mitochondrial DNA results in mitochondrial dysfunction. Proc Natl Acad Sci USA **88**: 10614-10618, 1991.
11. Wolf AM, Asoh S, Hiranuma H, et al. Astaxanthin protects mitochondrial redox state and functional integrity against oxidative stress. J Nutr Biochem **21**: 381-389, 2010.
12. Minamikawa T, Sriratana A, Williams DA, et al. Chloromethyl-X-rosamine (MitoTracker Red) photosensitizes mitochondria and induces apotosis in intact human cells. J Cell Sci **112**: 2419-2430, 1999.
13. Kamada T, Koizumi T, Tsujii M, et al. Clinical evaluation by double-blind trial of taurine for acute hepatitis. Sulfur-containing Amino Acid **3**: 223-235, 1980 (in Japanese).
14. Pion PD, Kittleson MD, Rogers QR, et al. Myocardial failure in cats associated with low plasma taurine: a reversible cardiomyopathy. Science **237**: 764-768, 1987.

Laboratory Investigation (2012) 92, 1100–1114

An inhibitor of transforming growth factor beta type I receptor ameliorates muscle atrophy in a mouse model of caveolin 3-deficient muscular dystrophy

Yutaka Ohsawa[1], Tadashi Okada[1], Shin-ichiro Nishimatsu[2], Masatoshi Ishizaki[3], Tomohiro Suga[3], Masahiro Fujino[1], Tatsufumi Murakami[1], Makoto Uchino[3], Kunihiro Tsuchida[4], Sumihare Noji[5], Atsushi Hinohara[6], Toshiyuki Shimizu[7], Kiyoshi Shimizu[6] and Yoshihide Sunada[1]

Skeletal muscle expressing Pro104Leu mutant caveolin 3 ($CAV3^{P104L}$) in mouse becomes atrophied and serves as a model of autosomal dominant limb-girdle muscular dystrophy 1C. We previously found that caveolin 3-deficient muscles showed activated intramuscular transforming growth factor beta (TGF-β) signals. However, the cellular mechanism by which loss of caveolin 3 leads to muscle atrophy is unknown. Recently, several small-molecule inhibitors of TGF-β type I receptor (TβRI) kinase have been developed as molecular-targeting drugs for cancer therapy by suppressing intracellular TGF-β1, -β2, and -β3 signaling. Here, we show that a TβRI kinase inhibitor, Ki26894, restores impaired myoblast differentiation *in vitro* caused by activin, myostatin, and TGF-β1, as well as $CAV3^{P104L}$. Oral administration of Ki26894 increased muscle mass and strength *in vivo* in wild-type mice, and improved muscle atrophy and weakness in the $CAV3^{P104L}$ mice. The inhibitor restored the number of satellite cells, the resident stem cells of adult skeletal muscle, with suppression of the increased phosphorylation of Smad2, an effector, and the upregulation of *p21* (also known as *Cdkn1a*), a target gene of the TGF-β family members in muscle. These data indicate that both TGF-β-dependent reduction in satellite cells and impairment of myoblast differentiation contribute to the cellular mechanism underlying caveolin 3-deficient muscle atrophy. TβRI kinase inhibitors could antagonize the activation of intramuscular anti-myogenic TGF-β signals, thereby providing a novel therapeutic rationale for the alternative use of this type of anticancer drug in reversing muscle atrophy in various clinical settings.

Laboratory Investigation (2012) **92,** 1100–1114; doi:10.1038/labinvest.2012.78; published online 14 May 2012

KEYWORDS: caveolin 3; limb-girdle muscular dystrophy 1C; muscular atrophy; myoblast; satellite cell; small-molecule kinase inhibitor; transforming growth factor-β type I receptor kinase

Muscle atrophy impairs the activities of daily living and is implicated in fatal outcomes in various diseases, including muscular dystrophy and cancer.[1,2] Recently, a growing number of transcription factors, membrane and cytoskeletal proteins, and cytokines have been found to participate in the molecular mechanisms leading to muscle atrophy, including caveolin 3 and myostatin.[3–8]

Caveolin 3, a muscle-specific integral membrane protein, forms flask-shaped invaginations of the plasma membrane known as caveolae, and regulates signal transduction pathways by binding specific lipid-modified signal molecules, including Ha-Ras, G protein-coupled receptors, Src-family kinases, and nitric oxide synthases.[9] Loss of caveolin 3 resulting from dominant-negative mutations in the *CAV3* gene causes autosomal dominant limb-girdle muscular dystrophy (LGMD) 1C.[9,10] We previously developed a transgenic mouse overexpressing Pro104Leu mutant caveolin 3 ($CAV3^{P104L}$) as a model of LGMD1C; these mice demonstrated myopathy characterized by muscle atrophy.[11] We found that the caveolin 3-deficient muscles in the transgenic mice showed activation

[1]Department of Neurology, Kawasaki Medical School, Okayama, Japan; [2]Department of Molecular and Developmental Biology, Kawasaki Medical School, Okayama, Japan; [3]Department of Neurology, Kumamoto University Graduate School of Medical Sciences, Kumamoto, Japan; [4]Division for Therapies against Intractable Diseases, Institute for Comprehensive Medical Science, Fujita Health University, Aichi, Japan; [5]Department of Life Systems, Institute of Technology and Science, The University of Tokushima Graduate School, Tokushima, Japan; [6]Drug Discovery Research Laboratories, Research Division, Kyowa Hakko Kirin, Shizuoka, Japan and [7]Research Planning Department, Research Division, Kyowa Hakko Kirin, Tokyo, Japan
Correspondence: Professor Y Sunada, MD, PhD, Department of Neurology, Kawasaki Medical School, 577 Matsushima, Kurashiki, Okayama 701-0192, Japan.
E-mail: ysunada@med.kawasaki-m.ac.jp

Received 30 August 2011; revised 23 February 2012; accepted 27 February 2012

of intramuscular transforming growth factor beta (TGF-β)-mediated signals, including myostatin, which is specifically expressed in skeletal muscle and negatively regulates muscle mass and growth.[5–8] However, the cellular pathobiology leading to muscle atrophy caused by the loss of caveolin 3 and activated intramuscular TGF-β signals remains to be elucidated.

Small-molecule compounds to antagonize TGF-β signals at membrane receptor serine/threonine kinases have recently been proposed as molecular-targeted drugs for cancer therapy.[12] Tumor cells in advanced stages become refractory to TGF-β-induced growth arrest, but often overexpress TGF-β1, -β2, and -β3.[13] TGF-β family members induce the epithelial–mesenchymal transition, immunosuppression, and angiogenesis, resulting in tumor growth and metastasis. Each member of the TGF-β family binds to a membrane serine/threonine kinase receptor, termed as a type II receptor, which then recruits a type I kinase receptor.[1,14] Seven different type I receptors, the activin receptor-like kinases 1–7 (ALK1–7), thus determine the intracellular signal specificity of the 33 members of the TGF-β family.[1,14] Small-molecule inhibitors of TGF-β type I receptor (TβRI) kinase were originally developed to compete with the binding of adenosine triphosphate to the kinase domain of ALK5, the type I receptor for TGF-β1-3.[12] TβRI kinase inhibitors have been found to suppress tumor enlargement and metastasis in the advanced stages of cancer in animals.[15–18] Notably, these inhibitors also suppress a similar kinase domain of ALK4, the type I receptor for activin, and potentially block ALK4/5, the type I receptor for myostatin.[1,12,19,20] However, the impact and clinical significance of TβRI kinase inhibitors on the skeletal muscle signaling of activin, myostatin, and TGF-β1-3 is unknown.

Considering the potential broad suppression profile of TβRI kinase inhibitors on the multiple intramuscular TGF-β signals, we postulated that these inhibitors could be used as optimal probes to explore the cellular mechanisms of how activated intramuscular TGF-β signals lead to muscle atrophy in caveolin 3-deficient muscular dystrophy. Alternatively, by suppressing the multiple anti-myogenic TGF-β signals, pharmacological intervention using this type of inhibitor would be expected to prevent muscle atrophy in caveolin 3-deficient mice. In the current study, we tested our hypothesis by examining the effects of TβRI kinase inhibitors on myogenesis *via* muscle precursor satellite cells, as well as myoblasts. The ability of an oral inhibitor to increase muscle mass, or to slow the progression of atrophy and weakness was further investigated in wild-type or caveolin 3-deficient mice, to investigate its potential in the future treatment of patients with muscular atrophy.

MATERIALS AND METHODS

Cell Lines and Reagents

A204 human rhabdomyosarcoma cells, HEK293 human embryonic kidney cells, and HaCaT human keratinocytes were maintained in Dulbecco's modified Eagle's medium (DMEM) containing 10% fetal bovine serum (FBS), 2 mM L-glutamine, 0.1 mM non-essential amino acids, and 50 μg/ml kanamycin. The pGL3-$(CAGA)_{12}$-luciferase reporter containing the TGF-β-sensitive Smad-binding sequence (CAGA) was kindly provided by Dr C-H Heldin (Uppsala University, Sweden).[21] Recombinant myostatin, activin A, and TGF-β1 (R&D Systems, Minneapolis, MN, USA) were prepared as 100 μg/ml stock solutions in 0.1% bovine serum albumin with 4 mM HCl. The small-molecule TβRI kinase inhibitors, Ki26894 (FW 374.40; Kyowa Hakko Kirin, Nagaizumi, Shizuoka, Japan), SB-431542 (FW 420.42; Sigma-Aldrich, St Louis, MO, USA), and LY-364947 (FW 327.30; Chemicon, Temecula, CA, USA) were dissolved and serially diluted from 10 mM to 1 μM in dimethyl sulfoxide as 1000-fold concentrated solutions. C2C12 myoblasts were maintained in growth medium comprising DMEM plus 10% FBS. The pMXs-IRES-GFP retroviral vector and the Plat-E packaging cells, and the antibody raised against M-cadherin, also known as cadherin 15 (CDH15), for satellite cell analysis, were kind gifts from T Kitamura (Institute of Medical Science, The University of Tokyo, Japan), and Drs Y Miyagoe-Suzuki and S-I Takeda (National Institute of Neuroscience, National Center of Neurology and Psychiatry, Japan), respectively.

Luciferase Assays

A204 cells or HEK293 cells were seeded on 12-well plates at 1.0×10^5 cells/well and maintained for 24 h, respectively. These cells were then co-transfected with the pGL3-$(CAGA)_{12}$-luciferase reporter gene. After 24 h, the medium was replaced with DMEM containing 10 ng/ml recombinant myostatin, 10 ng/ml activin A, or 6 ng/ml TGF-β1. The TβRI kinase inhibitors, Ki26894, SB-431542, or LY-364947 were also added to the culture medium. After an additional 24 h, cells were lysed with 1 × lysis buffer (Promega, Madison, WI, USA) and luciferase activity in the cell lysates was determined by a luciferase reporter assay system (Promega) using a MiniLumat LB 9506 luminometer (EG&G Berthold, Nashua, NH, USA) and was normalized to β-galactosidase activity. For the *ex-vivo* myostatin bioassay, sera from mice fed without or with Ki26894 were diluted four-fold (to 25%) with DMEM containing 10 ng/ml recombinant myostatin. The resulting mixture was added to HEK293 cells co-transfected with the pGL3-$(CAGA)_{12}$-luciferase reporter gene and pCMV-β-Gal.

In-Vitro Expression Assay for *p21* and *p15*

HaCaT human keratinocyte cells were seeded in 10-cm dishes at 1.0×10^6 cells/dish and maintained for 24 h, followed by incubation in serum-free medium for 2 h. The cells were then incubated with or without Ki26894 plus 10 ng/ml recombinant myostatin, 10 ng/ml activin A, or 6 ng/ml TGF-β1. Cellular RNA was extracted at the indicated times and the gene expression of *p21*, also known as *cyclin-dependent kinase inhibitor (Cdkn) 1a*, and *p15*, also known as *Cdkn1b*, was examined by northern blotting.

Construction of Retroviral Vectors

Mouse cDNAs for myostatin, activin A, and *TGF-β1* were cloned into retroviral vectors. The *NcoI–SalI* fragment of green fluorescent protein (*GFP*) cDNA in the original pMXs-IRES-GFP retroviral vector[22] was substituted with the Cherry cDNA fragment derived from the pmCherry-N1 plasmid vector (Clontech, Mountain View, CA, USA). One microgram of total RNA from mouse skeletal muscle was reverse transcribed with an oligo$(dT)_{12-18}$ primer and subjected to PCR using the following primers: myostatin, 5′-CGGGATC-CATGATGCAAAAACTG-3′ and 5′-CGGAATTCTCATGAG-CACCCAC-3′; activin A, 5′-CGGAATTCATGCCCTTGCTT TGG-3′ and 5′-CGCTCGAGCTAGGAGCAGCCAC-3′; *TGF-β1*, 5′-CGGAATTCATGCCGCCCTCGGGG-3′ and 5′-CGCTCGAGTCAGCTGCACTTGC-3′. The resulting PCR products were then cloned into the pMXs-IRES-Cherry vector using the appropriate restriction sites. The cDNA fragments of the Pro104Leu mutant caveolin 3 (ref. 5) were also ligated to the original vector.

In-Vitro Myogenic Differentiation Assays

Using the above retroviral vectors, we generated C2C12 cells expressing TGF-β family members, or Pro104Leu mutant caveolin 3, according to a method previously described.[22] Briefly, C2C12 myoblasts were maintained in growth medium comprising DMEM plus 10% FBS. Myogenic differentiation was initiated by placing 60% confluent cultures in differentiation medium comprising DMEM plus 2% horse serum with or without 10 nM Ki26894. Retrovirus vectors expressing TGF-β family members or mutant caveolin 3 were then transfected into Plat-E packaging cells. Supernatants containing retrovirus were passed through 0.45 μm filters. C2C12 cells were infected with the filtrates for 6 h and the medium was then replaced with differentiation medium. For immunocytochemical analysis, the cells were fixed and stained with anti-myosin heavy chain (MyHC) monoclonal antibody (mAb) (MY-32; Sigma-Aldrich), anti-muscle creatine kinase-M polyclonal antibody (N-13; Santa Cruz Biotechnology, Santa Cruz, CA, USA), or anti-myogenin mAb (F5D; Santa Cruz Biotechnology), followed by Alexa 488-conjugated anti-mouse or anti-goat IgG antibody (Invitrogen, Carlsbad, CA, USA). Lysates from C2C12 cells were resolved by SDS-polyacrylamide gel electrophoresis and transferred onto a polyvinylidene fluoride membrane. Immunoblot analysis was performed using MY-32.

Fusion Indices

The number of nuclei in mononucleated cells and myotubes defined as syncytia containing >3 nuclei were counted in four independent fields of 1 mm^2 ($n=5$). The fusion indices were calculated as ratios (%) of the total number of nuclei incorporated in myotubes.

Animals and Administration of Ki26894

Transgenic mice overexpressing the LGMD1C-causing Pro104Leu mutant caveolin 3 ($CAV3^{P104L}$)[9] under the control of 6.5 kb of the muscle creatinine kinase (*MCK*) gene promoter/enhancer sequences, including 3.3 kb upstream of exon 1, the complete intron 1 and exon 2 truncated just 5′ of the initiator methionine, were generated previously.[11] These mice demonstrated myopathy characterized by muscle atrophy and loss of caveolin-3, with increased intramuscular TGF-β signal.[5,6,11] Ki26894 was mixed with normal powdered food (CE-2; CLEA, Hamamatsu, Shizuoka, Japan) to a final concentration of 0.08%, and was orally administered to caveolin 3-deficient transgenic mice ($CAV3^{P104L}$) or control wild-type mice aged between 6 and 16 weeks, as described.[18] All animal experiments were performed at the Laboratory Animal Center and were approved by the Animal Research Committee of Kawasaki Medical School.

Immunohistochemical and Morphometric Analyses

Frozen quadriceps femoris muscles were transversely sectioned at the center of the muscles. The sections were fixed and stained using the anti-rat laminin α2 mAb (4H8-2; Sigma-Aldrich) followed by Alexa 488-conjugated anti-rat IgG antibody (Invitrogen). The areas of single myofibers in the quadriceps muscles ($n=20$; 250 myofibers per mouse) were measured on fluorescence images of laminin α2-stained sections using the two-color technique, as previously described.[5] To detect infiltration of inflammatory cells in muscles, sections were stained with a rat anti-mouse CD11b mAb (BD Pharmingen, San Diego, CA, USA).

For satellite cell analysis, the sections were stained with an anti-rabbit M-cadherin polyclonal antibody raised against the carboxyl-terminal region of mouse M-cadherin (Invitrogen) and an anti-rat laminin α2 mAb 4H8-2 (Sigma-Aldrich) followed by Alexa 488-conjugated anti-rabbit IgG and Alexa 594-conjugated anti-rat IgG Abs (Invitrogen). Myonuclei were post-stained with 4′,6-diamidino-2-phenylindole, DAPI (Vector Laboratories, Burlingame, CA, USA). The findings were confirmed using another anti-rabbit M-cadherin polyclonal antibody raised against amino acids 399–444 of mouse M-cadherin, as shown in Supplementary Figure 7.

Isolation of Single Myofiber and Attached Satellite Cells

We isolated single myofibers from the extensor digitorum longus (EDL) muscles of mice aged 16 weeks according to a previously described method.[23] Briefly, EDL muscles were digested in freshly prepared 0.5% type I collagenase (Worthington Laboratories, Freehold, NJ, USA) in DMEM. After gentle sucking of these muscle digests in and out of a wide-bore flame-polished Pasteur pipette, a single myofiber was isolated and placed individually on a coverslip precoated with 1 mg/ml Matrigel (BD Bioscience, San Jose, CA, USA). The single myofiber was fixed with 4% paraformaldehyde in PBS and stained with a rabbit anti-mouse caveolin-1 pAb

(BD Transduction Laboratories, Lexington, KY, USA), an anti-mouse caveolin-3 mAb (Santa Cruz), and an anti-mouse Pax7 mAb (GT), followed by labeling with Alexa 488-conjugated anti-rabbit and Alexa Fluor 594-conjugated anti-mouse IgG antibodies (Molecular Probe). Nuclei were post-stained with DAPI. Immunofluorescence images were captured using a laser scanning confocal microscope (TCS SP2; Leica Microsystems, Wetzlar, Germany) or a fully motorized inverse microscope (IX81, Olympus, Tokyo, Japan).

Vital Staining of Damaged Myofibers

To detect damaged myofibers, Evans Blue dye (EBD, 20 mg/ml in PBS) was injected into mice (0.15 ml/10 g body weight) intraperitoneally, basically according to a previously described method.[24] Mice were killed 24 h after injections. Skeletal muscles were sectioned and fluorescence images were evaluated under a fully motorized inverse microscope.

Muscle Performance

Mice grasping a wire mesh with their limbs were pulled horizontally by their tail until they lost their grip. Peak grip strength (g) was measured using an MK-380S automated Grip Strength Meter (Muromachi, Tokyo, Japan). The tetanic force of the tibialis anterior (TA) or diaphragm of mice at 16 weeks of age was measured essentially as previously described.[25] Briefly, the TA or diaphragm was quickly excised and the peripheral tendons were secured with a 5-0 silk suture. Both ends of the muscle were fixed using a tissue clamp (B-small; Natsume, Tokyo, Japan). The muscle was vertically mounted in a chamber that was perfused with oxygen-saturated Ringer's solution and maintained at 25 °C. The muscle was then connected to a UL-50GR force transducer (Minebea), and an MM-3 length servosystem (Narishige, Tokyo, Japan). The muscle was stimulated through a pair of platinum plates attached at both sides of the chamber using an SEN-3401 electronic stimulator (Nihon Kohden, Tokyo, Japan). Tetanic force was recorded and analyzed using a PowerLab system and LabChart v6 software (ADInstruments, Colorado Springs, CO, USA). The length of the muscle fibers was incrementally adjusted using a micropositioner until the maximal twitch force response was obtained (optimal fiber length). The maximal tetanic force was assessed at a stimulation frequency of 150 Hz delivered in 1000 ms trains with 2 min intervals between trains. After obtaining three measurements, the attached bone and sutures were removed and the muscle was weighed. The muscle cross-sectional area was calculated using the formula: muscle wet weight (in mg)/optimal fiber length (in mm) × 1.056 (in mg/mm^3). Specific tetanic forces (maximal tetanic force/cross-sectional area) of the muscle were determined using the estimated cross-sectional area.

RT-PCR and Northern Blotting

Total RNAs from mouse skeletal muscle or HaCaT cells were fractionated on northern gels, and probed with labeled cDNAs for mouse *p21* (nucleotides (nt) 1–255), mouse *p15* (nt 32–385), mouse *18S* rRNA (nt 1–453), human *p21* (nt 1–255), or human *p15* (nt 508–921).

Smad2 Phosphorylation Analysis

Skeletal muscle from 16-week-old mice was homogenized in 10 volumes (w/v) of a buffer consisting of 50 mM Tris-HCl (pH 7.4), 100 mM NaCl, 1 mM EDTA, 5 mM β-mercaptoethanol, 0.1 mM PMSF, and 1 mM benzamidine. The crude extracts were resolved by SDS-polyacrylamide gel electrophoresis and transferred onto polyvinylidene fluoride membranes. Immunoblot analysis was performed using rabbit anti-mouse Smad2 or phosphorylated Smad2 (p-Smad2) (Ser465/467) antibodies (Cell Signaling Technology, Danvers, MA, USA).

Statistics

Paired observations were statistically analyzed using one-way analysis of variance followed by Bonferroni's test. *P*-values <0.05 were considered statistically significant.

RESULTS

TβRI Kinase Inhibitors Broadly Suppress the *In-Vitro* Transcriptional Activities of TGF-β Family Members

To investigate whether TβRI kinase inhibitors can suppress TGF-β signals other than TGF-β1-3 *in vitro*, we tested three inhibitors: SB-431542, LY-364947, and Ki26894.[17–20] A204 human rhabdomyosarcoma cells or HEK293 human embryonic kidney cells were transfected with pGL3-$(CAGA)_{12}$-luciferase, a TGF-β-sensitive Smad-responsive luciferase reporter gene.[21] Stimulation of these cells with recombinant myostatin, activin A, or TGF-β1 caused a significant increase in luciferase activity above the basal level (A204: Figure 1a–c; HEK293: Figure 1d–f). The addition of an individual inhibitor to the culture media suppressed luciferase activity in a dose-dependent manner. The intracellular signal specificity of myostatin, activin A, or TGF-β1 is determined by the recruitment of ALK4/5.[1] Thus, these TβRI kinase inhibitors can suppress the intracellular signaling of myostatin through ALK4/5, activin A through ALK4, and TGF-β1 through ALK5. In A204 cells, the three inhibitors suppressed myostatin, activin A, or TGF-β1 comparably, whereas in HEK293 cells, Ki26894 inhibited myostatin ~15-fold more potently than either SB-431542 or LY-364947 with half-maximal inhibitory concentration values of 7, 100, and 100 nM, respectively. We selected Ki26894 as a representative inhibitor for subsequent experiments.

We further investigated the effects of Ki26894 on TGF-β-induced gene expression of the cyclin-dependent kinase (CDK) inhibitors, *p21* and *p15* in HaCaT human keratinocyte cells, a cell line in which the intracellular signaling pathways activated by different members of the TGF-β family have been characterized in detail.[26] Myostatin time dependently induced the expression of *p21*, but not of *p15*, while Ki26894 suppressed *p21* upregulation (Figure 1d). Ki26894

also blocked p21 expression induced by activin A and TGF-β1. Thus, this TβRI kinase inhibitor suppressed the common intracellular signal pathways leading to *p21* upregulation that are induced by the different members of the TGF-β family.

Ki26894 Reverses Impaired Myoblast Differentiation *In Vitro* Caused by TGF-β1, Activin, and Myostatin

Myostatin suppresses the differentiation of C2C12 myoblasts exposed to low-serum conditions.[27] Using an efficient

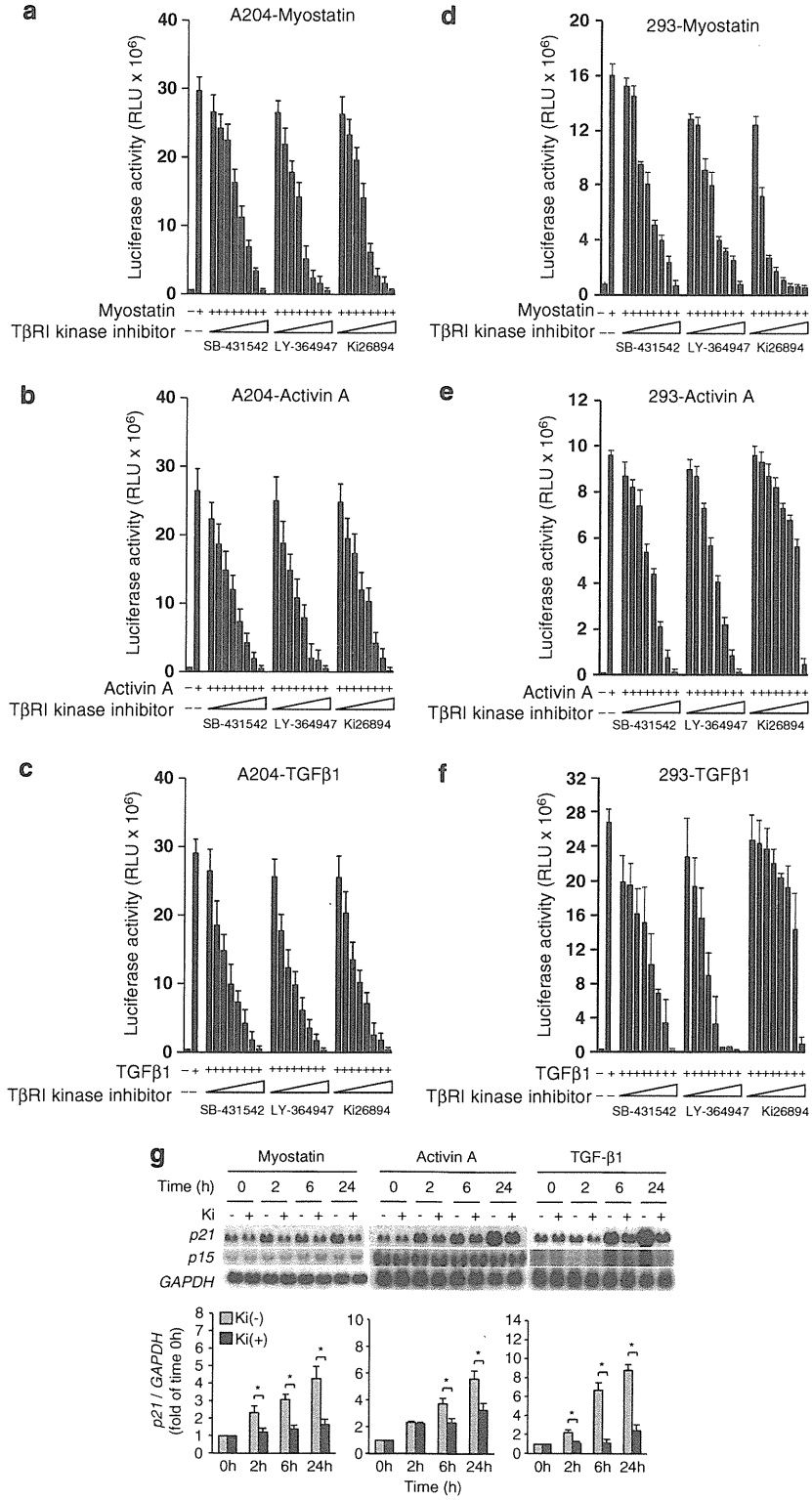

retrovirus-mediated gene transfer system,[22] we assessed the effect of Ki26894 on the differentiation of C2C12 myoblasts expressing TGF-β1 or activin A, as well as myostatin. Transferring C2C12 myoblasts expressing an empty vector from high-serum (growth) to low-serum (differentiation) media caused them to fuse and form multinucleated myotubes. We

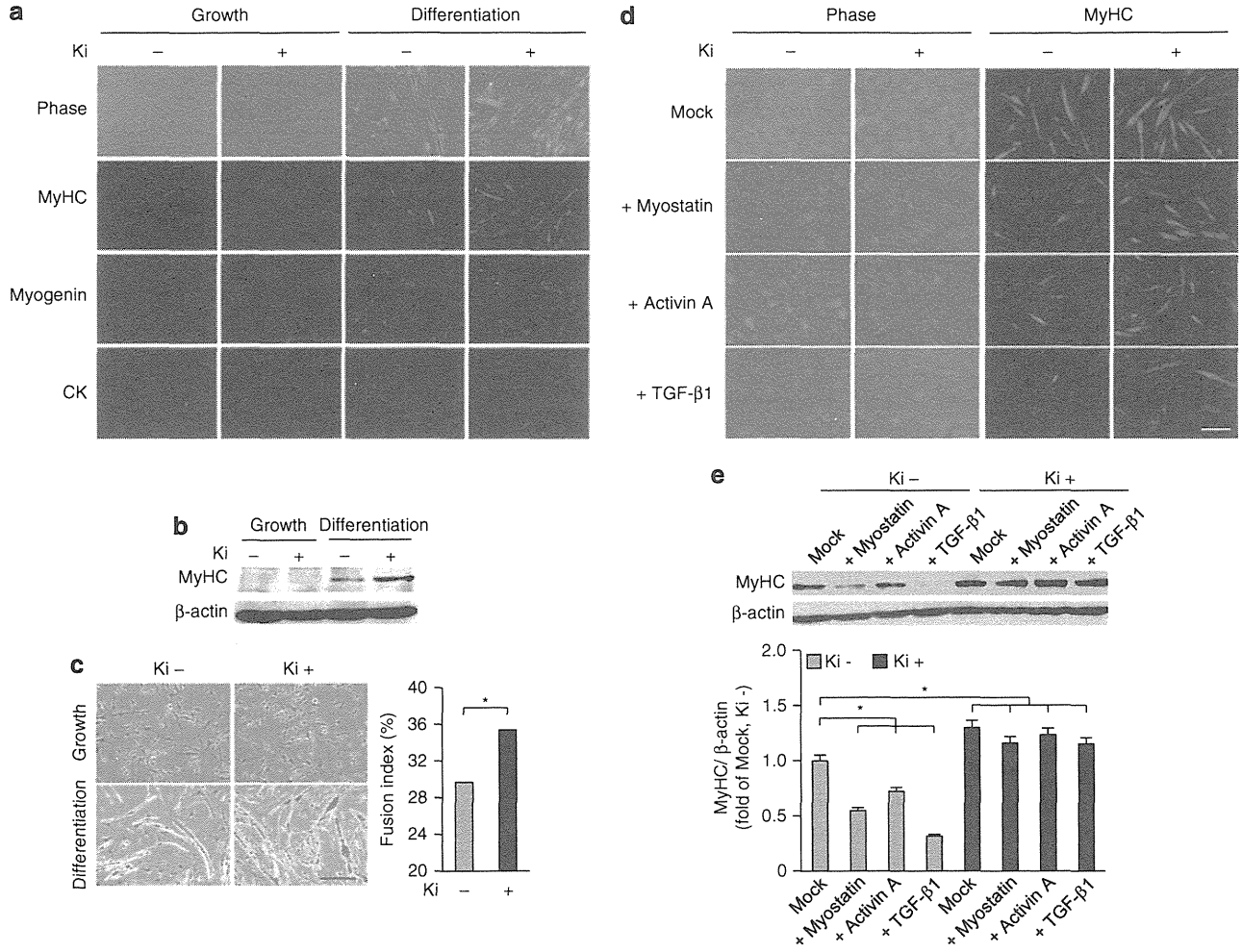

Figure 2 The TβRI kinase inhibitor Ki26894 (Ki) reverses the impaired *in-vitro* myogenesis caused by myostatin, activin A, and TGF-β1. (**a**) C2C12 myoblasts expressing an empty vector were grown in DMEM containing 10% FBS (growth medium) and then differentiated in DMEM containing 2% horse serum (differentiation medium), without (–) or with (+) 10 nM Ki26894 for 6 days. The cells were then stained with myogenic differentiation markers: MyHC, myogenin, or CK. Phase-contrast and fluorescent images. Bar, 5 μm. (**b**) Immunoblot analysis of MyHC in lysates from C2C12 cells expressing an empty vector in growth medium or differentiation medium without (–) or with (+) Ki26894. (**c**) Giemsa and Wright-stained images of C2C12 cells expressing an empty vector in growth medium or differentiation medium without (–) or with (+) Ki26894 (left). Fusion indices of these cells following the addition of 10 nM Ki26894 were calculated in triplicate as the percent of the total nuclei in myotubes/mm^2 (right). Values are means ± s.d. ($n = 5$). *$P < 0.05$. (**d**) C2C12 myoblasts expressing empty vector (mock), myostatin, activin A, or TGF-β1 were cultured in differentiation medium without (–) or with (+) 10 nM Ki26894 for 6 days and then stained with MyHC. Phase-contrast (left) and fluorescent (right) images are shown. Bar, 15 μm. (**e**) Analysis of MyHC protein expression in lysates from C2C12 cells expressing empty vector (mock), myostatin, activin A, or TGF-β1 at 6 days after differentiation without (–) or with (+) Ki26894 (upper). Densitometric analysis of the MyHC/β-actin ratio in differentiated C2C12 cells (lower). Values are mean ± s.d. fold increases compared with untreated C2C12 lysates expressing empty vector (mock) ($n = 5$). *$P < 0.05$.

Figure 1 TβRI kinase inhibitors suppress myostatin-, activin A-, and TGF-β1-induced transcriptional activities *in vitro*. A204 human rhabdomyosarcoma cells (left; **a**–**c**) or HEK293 human embryonic kidney cells (right; **d**– **f**) were co-transfected with both the Smad-responsive luciferase reporter gene pGL3-$(CAGA)_{12}$-luciferase and pCMV-β-Gal. Cells were stimulated 24 h later with 10 ng/ml of myostatin (**a**, **d**), 10 ng/ml of activin A (**b**, **e**), or 6 ng/ml of TGF-β1 (**c**, **f**) and simultaneously exposed to increasing concentrations (1, 10, 50, 100, 250, 500, 1000, or 10 000 nM; indicated by triangles) of SB-431542 (left), LY-364947 (center), or Ki26894 (right). Luciferase activity was measured and normalized to β-Gal activity. Values are means ± s.d. ($n = 10$). RLU, relative luminescence units. (**g**) HaCaT human keratinocytes were cultured in medium containing serum. After preincubation in serum-free medium for 2 h, the cells were stimulated with 10 ng/ml recombinant myostatin (left), 10 ng/ml activin A (center), or 6 ng/ml TGF-β1 (right) (upper). Cells were then maintained without (–) or with (+) 10 nM Ki26894 (Ki). The gene expression levels of *p21* or *p15* in cells at 0, 2, 6, and 24 h after stimulation were examined by northern blotting. Densitometric analysis of the *p21/GAPDH* ratio (lower). Values are mean ± s.d. fold increases relative to untreated cells at time 0 ($n = 7$). *$P < 0.05$.

then stained the cells with antibodies against MyHC, myogenin, and creatine kinase (CK), and measured the fusion indices (Figure 2a–c). Adding Ki26894 to the culture media enhanced myoblast fusion and myotube formation. On the other hand, myotube formation was impaired in C2C12 myoblasts expressing myostatin, activin A, or TGF-β1, compared with controls harboring an empty vector (Figure 2d and e). Notably, Ki26894 reversed the impaired myotube formation induced by these TGF-β family members. Immunoblotting analyses showed that Ki26894 restored the reduced protein expression of MyHC in C2C12 myoblasts. These findings indicate that TβRI kinase inhibitors enhance myoblast differentiation *in vitro* by suppressing the activity of several members of the anti-myogenic TGF-β family members, including activin, or TGF-β1, as well as myostatin.

Ki26894 Reverses Reduced Myotube Formation by Forced Expression of Pro104Leu Mutant Caveolin 3

We previously showed that caveolin 3 binds and suppresses ALK4/5 in COS7 monkey kidney cells by forced expression of these molecules using plasmid vectors.[5] Moreover, other groups have reported that expression of a *CAV3* antisense RNA, or a Pro104Leu dominant-negative mutant *CAV3* cDNA suppressed the differentiation of C2C12 myoblasts into myotubes under low-serum conditions.[28,29] We thus expressed the Pro104Leu dominant-negative mutant *CAV3* cDNA in C2C12 cells using the above retroviral system, to explore the molecular significance of caveolin 3 and TGF-β signals in myoblast differentiation. Similarly to the results of the TGF-β expression, myotube formation was impaired in C2C12 myoblasts overexpressing Pro104Leu mutant caveolin 3, compared with controls (Figure 3a–c). Importantly, Ki26894 reversed the impaired myotube formation induced by the mutant caveolin 3. TβRI kinase inhibitors thus could reverse myotube formation by suppressing the enhanced intracellular TGF-β signals resulting from a dominant-negative caveolin 3 mutation.

Administration of an Oral TβRI Kinase Inhibitor Enhances Myogenesis *In Vivo* in Wild-Type Mice

Before starting systemic administration of Ki26894, we determined its bioavailability against myostatin activity using an *ex-vivo* bioassay system. Ki26894 was orally administered in the food to 10-week-old wild-type mice as previously described.[18] Sera from 12-week-old wild-type mice fed with or without Ki26894 for 2 weeks were added to the culture media of HEK293 cells transfected with a luciferase reporter gene ($n = 10$; Supplementary Figure 1). Recombinant myostatin-induced luciferase activity was decreased to 19% by adding sera from Ki26894-fed mice to the culture media to a final concentration of 25%. Thus, the sera in physiological conditions (50% in blood) should completely suppress myostatin activity. Therefore, we administered Ki26894 orally to the mice at a concentration of 0.08% in their food.

Ki26894 was orally administered in powdered food to wild-type mice starting at 6 weeks of age. The body weight of the mice fed with or without Ki26894 was monitored until 16 weeks, when the mice were killed for further analysis. Body weight, peak grip strength force, muscle weight, and single myofiber area (SMA) were larger in mice fed with Ki26894 compared with those not fed with Ki26894, suggesting enhanced myogenesis *in vivo* (Supplementary Figure 2).

Oral Administration of Ki26894 Rescues Muscle Atrophy in Caveolin 3-Deficient Mice

We next administered Ki26894 to an atrophic caveolin 3-deficient muscular dystrophy model mouse ($CAV3^{P104L}$), because we previously demonstrated that elevated intramuscular TGF-β signals led to muscle atrophy in these mice.[5] The mice fed with Ki26894 from 9–10 to 16 weeks of age were significantly heavier than those that did not receive Ki26894 ($n = 20$; Figure 4a). We did not detect any adverse effects in the mice fed with Ki26894 at any time point until 16 weeks, and no significant pathological abnormalities were found at the end of the experiments, including in the ovary where suppression of activin was reported to cause a reproductive defect[30] (Supplementary Figure 6). The observation of skinned hind-limb muscles showed that Ki26894 ameliorated muscle atrophy compared with the muscles of untreated mice (Figure 4b). Ki26894 also increased muscle weight in $CAV3^{P104L}$ mice (Figure 4c). At 16 weeks of age, H&E-stained sections of quadriceps femoris muscles from both $CAV3^{P104L}$ and wild-type mice were examined. As we reported previously,[5,11] $CAV3^{P104L}$ mouse muscle (Figure 4d, upper) showed marked reduction of myofiber size, compared with wild-type mouse muscle (Figure 4d, lower). Conversely, Ki26894 treatment appeared to alleviate the reduced myofiber size in the $CAV3^{P104L}$ mice. Morphometric analyses showed that the SMA in the muscles was significantly greater in $CAV3^{P104L}$ mice treated with Ki26894 than in untreated $CAV3^{P104L}$ mice (males, 929.7 ± 320.7 *vs* $559.4 \pm 219.4\ \mu m^2$; females, 768.3 ± 335.1 *vs* $538.3 \pm 208.1\ \mu m^2$; both $P < 0.05$; Figure 4e). Consistently, the SMA in Ki-treated wild-type mice was also significantly increased compared with that in untreated wild-type mice (males, 3779.1 ± 762.9 *vs* $2937.7 \pm 607.7\ \mu m^2$; females, 3389.8 ± 756.5 *vs* $2685.4 \pm 746.5\ \mu m^2$; both $P < 0.05$; Supplementary Figure 2). Thus, long-term administration of Ki26894 induces postnatal myofiber hypertrophy as shown by the increase in mean SMA in $CAV3^{P104L}$ mice (males, $\times 1.48$; females, $\times 1.42$) and wild-type mice (males, $\times 1.28$; females, $\times 1.26$).

We further examined the effects of Ki26894 on muscle histology other than myofiber size, including the number of EBD-positive necrotic myofibers (Supplementary Figure 3), infiltration of CD11b-positive inflammatory cells (Supplementary Figure 4a) and Masson's trichrome-positive fibrous tissue replacement (Supplementary Figure 4b), and the number of centrally nucleated regenerative myofibers (Supplementary Figure 5). These changes were far less common in $CAV3^{P104L}$ mice than in dystrophin-deficient

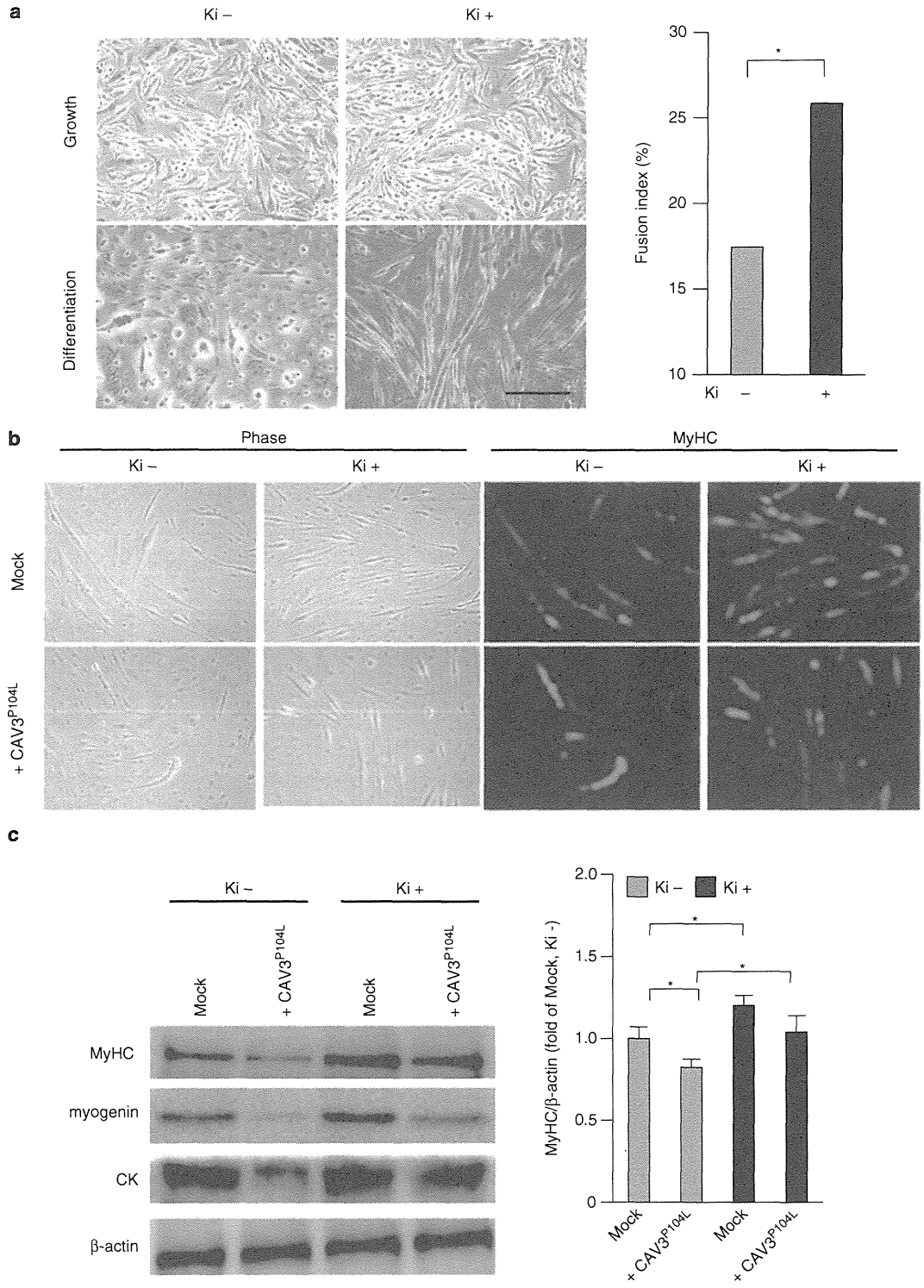

Figure 3 The TβRI kinase inhibitor Ki26894 (Ki) restored the impaired *in-vitro* myogenesis caused by forced expression of Pro104Leu dominant-negative mutant caveolin 3 ($CAV3^{P104L}$). (**a**) Giemsa and Wright-stained images of C2C12 cells expressing Pro104Leu mutant caveolin 3 in growth medium or differentiation medium without (−) or with (+) Ki26894 (left). Fusion indices of these cells following the addition of 10 nM Ki26894 were calculated in triplicate as the percent of the total nuclei in myotubes/mm^2 (right). Values are means ± s.d. ($n = 5$). *$P < 0.05$. (**b**) C2C12 myoblasts expressing empty vector (mock), or Pro104Leu mutant caveolin 3 were differentiated without (−) or with (+) 10 nM Ki26894 for 6 days and then stained with MyHC. Phase-contrast (left) and fluorescent (right) images are shown. Bar, 15 μm. (**c**) Protein expression of MyHC, myogenin, and CK in lysates from C2C12 cells expressing empty vector (mock) or Pro104Leu mutant caveolin 3 ($CAV3^{P104L}$) at 6 days after differentiation without (−) or with (+) Ki26894 (left). Densitometric analysis of the MyHC/β-actin ratio in differentiated C2C12 cells (right). Values are mean ± s.d. fold increases compared with untreated C2C12 lysates expressing empty vector (mock) ($n = 5$). *$P < 0.05$.

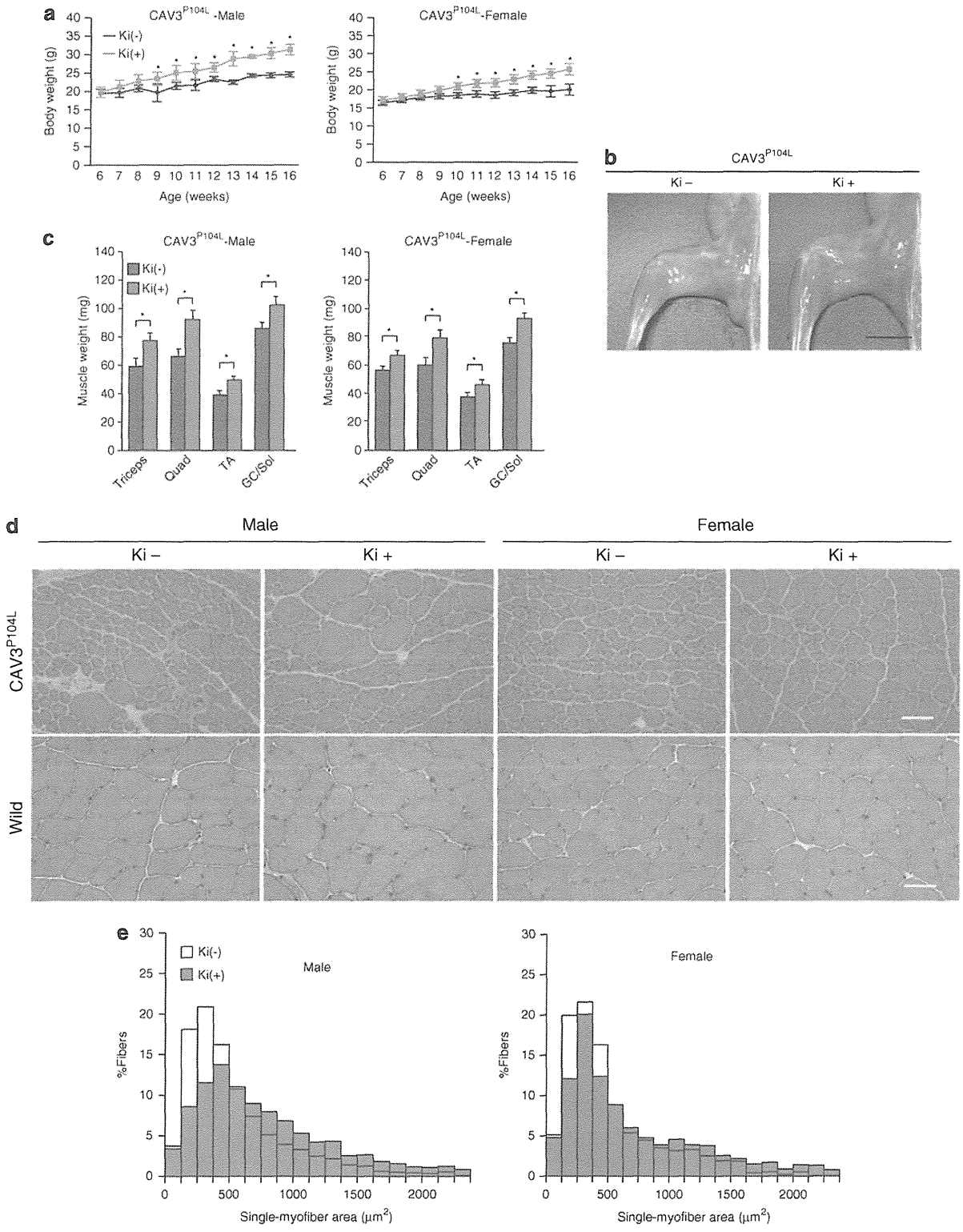

Figure 4 Oral administration of Ki26894 (Ki) ameliorates muscular atrophy and myofiber hypotrophy in caveolin 3-deficient mice. (**a**) Comparison of body weight at 6 and 16 weeks of age between CAV3^{P104L} mice fed without (−) or with (+) Ki26894. Values are means ± s.d. ($n = 20$). *$P < 0.05$. (**b**) Appearance of skinned hind limbs from 16-week-old mice fed without (−) or with (+) Ki26894. Scale bar, 5 mm. (**c**) Comparison of muscle weight in 16-week-old CAV3^{P104L} mice fed without (−) or with (+) Ki26894. Triceps, triceps brachii; Quad, quadriceps femoris; GC/Sol, gastrocnemius/soleus. Values are means ± s.d. ($n = 10$). *$P < 0.05$. (**d**) Histological analysis of the quadriceps femoris in 16-week-old CAV3^{P104L} mice (upper) and wild-type mice (lower) fed without (−) or with (+) Ki26894. Scale bar, 50 μm. (**e**) Distribution of SMAs of the quadriceps femoris from 16-week-old CAV3^{P104L} mice ($n = 20$; 250 myofibers were assessed in each mouse).

mdx mice, thereby making it difficult to compare Ki26894-treated and Ki26894-untreated muscles. However, we did observe a statistically significant increase in the number of centrally nucleated fibers in Ki26894-treated CAV3^{P104L} mouse muscles, suggesting an increase in the amount of muscle regeneration induced by Ki26894.

Peak grip strength force was also greater in Ki26894-treated mice than in untreated mice ($n = 20$; Figure 5a). As ex-

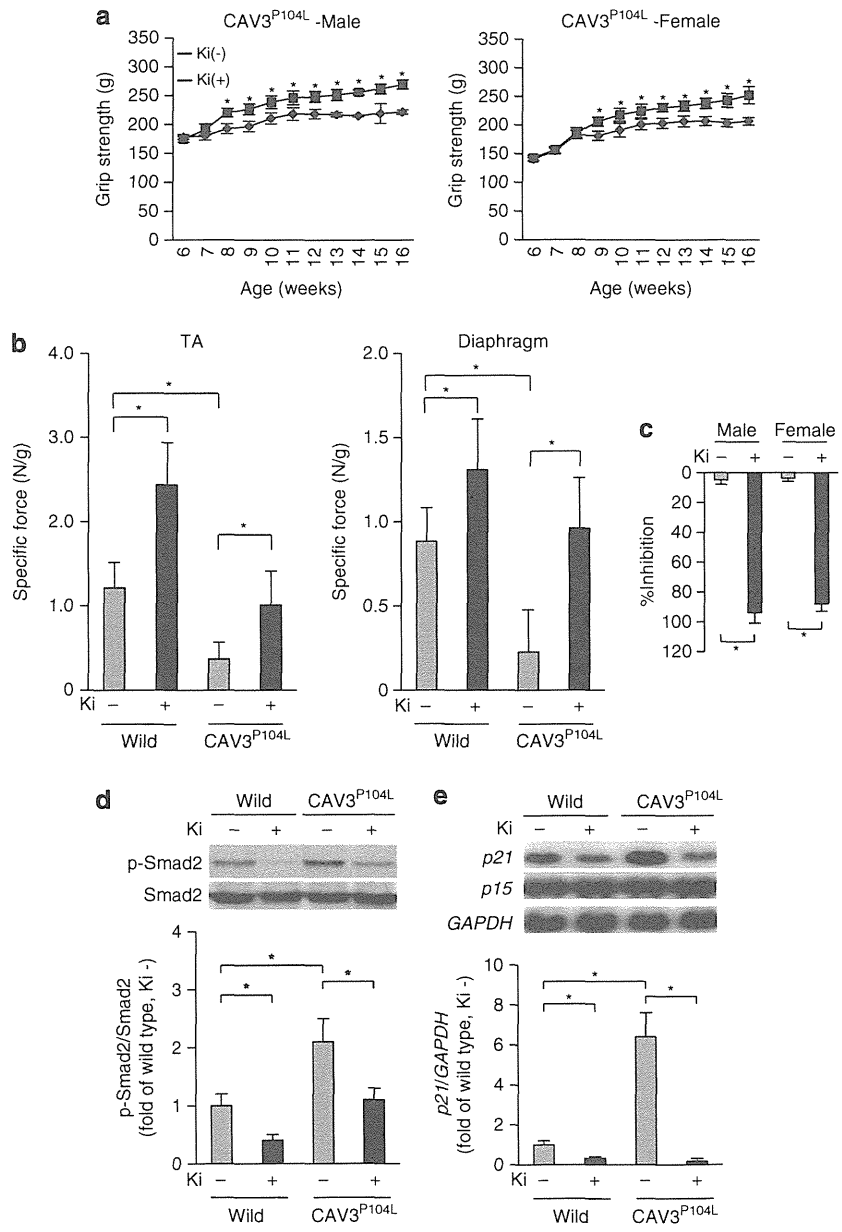

Figure 5 Oral administration of Ki26894 (Ki) rescues muscular weakness in caveolin 3-deficient mice by suppressing intramuscular TGF-β signaling. (**a**) Comparison of peak grip strength (g) at 6 and 16 weeks of age between CAV3^{P104L} mice fed without (−) or with (+) Ki26894. Values are means ± s.d. ($n = 20$). *$P < 0.05$. (**b**) Specific force of the TA or diaphragm from CAV3^{P104L} (left) and wild-type (right) mice at 16 weeks of age fed without (−) or with (+) Ki26894. Maximal tetanic force was assessed at the stimulation frequency of 150 Hz delivered in 1000 ms bursts. Values are means ± s.d. ($n = 10$). *$P < 0.05$. (**c**) Inhibition rate (%) of *ex-vivo* myostatin activity by Ki26894. Sera from 12-week-old CAV3^{P104L} mice fed without (−) or with (+) Ki26894 were diluted four-fold (to 25%) and added to the culture media of HEK293 cells co-transfected with pGL3-$(CAGA)_{12}$-luciferase and pCMV-β-Gal (internal control), followed by stimulation with 10 ng/ml myostatin. Luciferase activities were measured and normalized to β-Gal activity. Recombinant myostatin-induced luciferase activity was decreased by over 80% by adding the four-fold-diluted sera from mice of both sexes fed with Ki26894. Values are means ± s.d. ($n = 10$). *$P < 0.05$. (**d**) Immunoblot analysis of total Smad2 and p-Smad2 in crude muscle homogenates from wild-type and CAV3^{P104L} mice fed without (−) or with (+) Ki26894 (upper). p-Smad2/Smad2 ratios determined by densitometric analysis (lower). Values are mean ± s.d. fold increases with respect to wild-type mice ($n = 7$). *$P < 0.05$. (**e**) Northern blot analysis of *p21* and *p15* in muscles from CAV3^{P104L} mice fed without (−) or with (+) Ki26894 (upper). Densitometric analysis of the *p21/GAPDH* ratio (lower). Values are mean ± s.d. fold increases compared with untreated wild-type mice ($n = 7$). *$P < 0.05$.

pected, the specific force of the TA or diaphragm muscles was significantly lower in CAV3^{P104L} mice than in wild-type mice ($n=7$; Figure 5b). Oral Ki26894 increased muscle-specific force both in CAV3^{P104L} mice and in wild-type mice. We also found that serum myostatin activity was significantly reduced in Ki26894-treated CAV3^{P104L} mice compared with that in untreated mice at 15 weeks of age (Figure 5c).

Ki26894 Decreases the Intramuscular TGF-β Signal and Increases the Number of Satellite Cells *In Vivo*

To investigate the intramuscular TGF-β signal, we examined the levels of p-Smad2, its intracellular effector, in crude muscle homogenates ($n=7$; Figure 5d). The amounts of total Smad2 protein were comparable in wild-type and CAV3^{P104L} mice, with or without Ki treatment, whereas the level of p-Smad2 was significant increased in CAV3^{P104L} mice compared with wild-type mice. Ki treatment significantly reduced p-Smad2 levels in both lines of mice. We further investigated the expression of p21 and p15 in the skeletal muscle of CAV3^{P104L} mice to determine the effects of Ki26894 on intramuscular signaling ($n=7$; Figure 5e). The mRNA expression of *p21* was increased in CAV3^{P104L} mice compared with wild-type mice, suggesting enhanced intramuscular TGF-β signaling caused by loss of caveolin 3. Importantly, oral Ki26894 administration decreased *p21* expression in both wild-type and CAV3^{P104L} mice. In contrast, *p15* expression was not affected by oral administration of Ki26894. These results are consistent with our *in-vitro* findings that TβRI kinase inhibitors suppress intracellular signaling pathways activated by members of the anti-myogenic TGF-β family.

Muscle precursor satellite cells reside beneath the basal lamina of the myofibers, where they have important roles in postnatal muscle growth as resident stem cells in adult skeletal muscle.[31] We evaluated satellite cells in the quadriceps femoris muscles of CAV3^{P104L} mice compared with wild-type mice by immunostaining for the marker protein M-cadherin. At both time points (6, 10, or 24 weeks of age), the number of M-cadherin-positive satellite cells in muscles from the caveolin 3-deficient transgenic mice was reduced compared with that in the wild-type mice, accompanied by a reduction in myofiber size (Figure 6a). Because the number of satellite cells in skeletal muscle is known to reduce with age,[31] we counted the number of satellite cells per 100 myofibers or per 100 myonuclei from the quadriceps femoris muscles of mice at three time points (6, 10, or 24 weeks of age; $n=7$, Figure 6b). Compared with the wild-type mice, the caveolin 3-deficient transgenic mice showed a significant reduction in the number of satellite cells at all time points, not only per 100 myofibers, but also per 100 myonuclei. Thus, satellite cell reduction could contribute to the cellular mechanism leading to muscle atrophy in caveolin 3-deficient mice. Consistently, at 16 weeks of age, we found fewer satellite cells in the quadriceps femoris muscles of CAV3^{P104L} mice than in wild-type mice ($n=7$; Figure 6c and d, left). Conversely, Ki26894 increased the numbers of satellite cells in both caveolin 3-deficient mice and wild-type mice ($n=7$; Figure 6c and d, right). These findings were confirmed using another M-cadherin antibody ($n=7$; Supplementary Figure 7). TβRI kinase inhibitors thus increased resident stem cells in both caveolin 3-deficient and normal adult muscle.

Caveolin 1, another isoform of caveolins, was reported to be expressed in M-cadherin-positive satellite cells.[32] To confirm this finding, we stained single myofibers isolated from the EDL muscles of wild-type mice. Because the above two anti-M-cadherin antibodies used in histochemistry showed weak immunoreactivities on satellite cells attached to isolated single myofibers (data not shown), we used an antibody against Pax7, another marker of satellite cells. An anti-caveolin-1 antibody stained the regions surrounding Pax-7-positive mononucleated cell attached to a single myofiber from wild-type mice (Supplementary Figure 7b). Double immunostaining for caveolin 1 and caveolin 3 showed caveolin 1-positive cells located outside of the caveolin 3-positive sarcolemma, confirming the report that caveolin 1 is expressed in the cytoplasm and/or the plasma membrane of satellite cells, whereas caveolin 3 is expressed in the sarcolemma[32] (Supplementary Figures 7c and 8). Using the antibody against caveolin 1, we analyzed satellite cells attached to isolated single myofiber from CAV3^{P104L} and wild-type mice fed with or without Ki26894 (Figure 6e). Single myofiber isolated from muscles of CAV3^{P104L} mice had a reduced number of caveolin 1-positive satellite cells, compared with that of wild-type mice. Ki treatment appeared to alleviate the reduced number of satellite cells and the reduced size of myofiber in CAV3^{P104L} mice. Quantitative analyses revealed that the numbers of satellite cells per 100 myofibers significantly increased following Ki treatment in isolated myofibers from both lines of mice ($n=7$).

DISCUSSION

A growing number of molecules have recently been demonstrated to participate in the molecular mechanisms leading to skeletal muscle atrophy. However, no effective pharmacological intervention is currently available to improve muscle atrophy, except oral steroids, which are of limited efficacy.[3,4] Small-molecular inhibitors targeting membrane receptor tyrosine or serine/threonine kinases have been highlighted, and in part, are clinically available as molecular-targeting agents for cancer therapy.[33] In the present study, using such an inhibitor of TβRI kinase as an optimal probe, we found that the decrease in muscle precursor satellite cells and impairment of myoblast differentiation that accompanied activation of the TGF-β signaling pathway led to muscular atrophy in a caveolin 3-deficient mouse model. By suppression of multiple anti-myogenic TGF-β signals, oral small-molecule TβRI inhibitors could become an alternative, rationally designed, molecular-targeting agent for treating muscular atrophy in various clinical settings besides caveolin 3 deficiency.

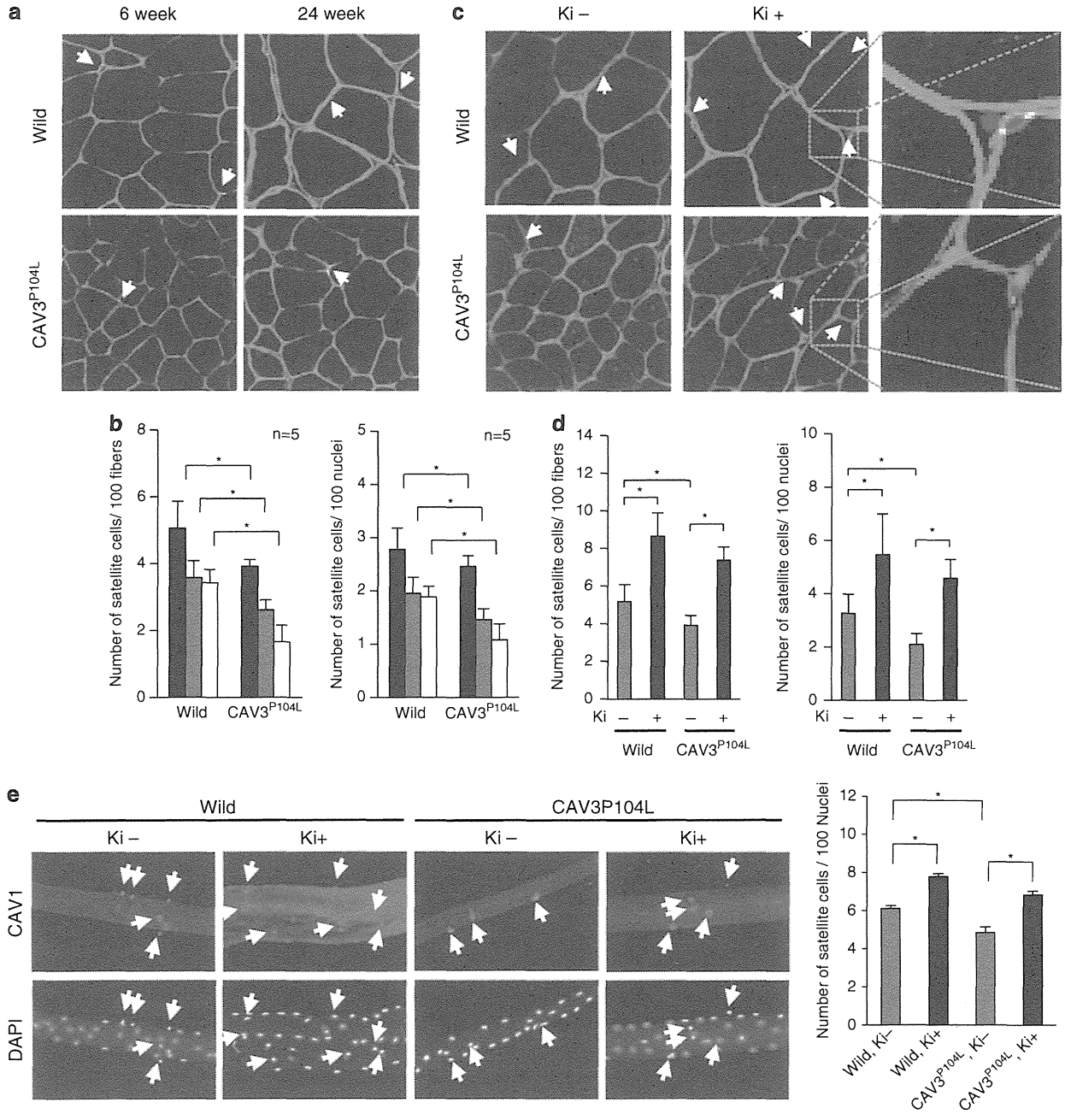

Figure 6 Ki26894 (Ki) reverses the reduced number of satellite cells in caveolin 3-deficient LGMD1C model mice. (**a**) Immunohistochemical analysis of satellite cells of the quadriceps femoris from 6- or 16-week-old wild-type (Wild) or CAV3^{P104L} mice using an antibody raised against the carboxyl-terminal region of mouse M-cadherin. At both ages, the number of M-cadherin-positive satellite cells in muscles from caveolin 3-deficient transgenic mice was decreased compared with that in wild-type mice. M-cadherin, laminin $\alpha 2$, and the nuclei are stained green, magenta, and blue, respectively. White arrow, M-cadherin-positive satellite cells residing beneath the basal lamina. Scale bar, 50 μm. (**b**) The number of satellite cells/100 myofibers (left) or 100 myonuclei (right) in quadriceps femoris muscles from wild-type or CAV3^{P104L} mice was counted at 6 (black), 10 (gray), or 16 (white) weeks of age ($n = 7$; 1000 myofibers or myonuclei were assessed for each mouse). Values are means ± s.d., $n = 7$. *$P < 0.05$. (**c**) Satellite cells of quadriceps femoris muscles from 16-week-old wild-type or CAV3^{P104L} mice fed with (+) or without (–) Ki26894. Oral Ki26894 reversed the reduced number of satellite cells in CAV3^{P104L} mice and increased the number of satellite cells in CAV3^{P104L} mice. Scale bar, 50 μm. The enlarged images of the boxed regions included satellite cells are shown on the right side of the original picture. (**d**) The number of satellite cells/100 myofibers (left) or 100 myonuclei (right) in quadriceps femoris muscles from wild-type or CAV3^{P104L} mice, fed without (gray) or with (red) Ki26894. *$P < 0.05$. (**e**) Fluorescence images of caveolin 1, a satellite cell marker protein (green), and nuclei (blue), in a single myofibers isolated from the EDL muscles of wild-type and CAV3^{P104L} mice aged 16 weeks. The white arrow indicates caveolin 1-positive satellite cells attached to the myofiber (left). Quantification of the number of caveolin 1-positive satellite cells attached to a single myofiber (right). Number of satellite cells per 100 myonuclei in a single myofiber from the EDL muscles of 16-week-old mice. Ki treatment significantly increased the number of satellite cells in wild-type mice and alleviated the reduction in the number of satellite cells in CAV3^{P104L} mouse myofibers. Data are mean values ± s.d. ($n = 5$; 10 myofibers were assessed for each mice). *$P < 0.05$.